Electronic Supplementary Material (ESI) for ChemComm.

Electronic Supplementary Information for:

C–F activation Reactions at Germylium Ions: Dehydrofluorination of Fluoralkanes

M. Talavera, G. Meißner, S. G. Rachor, T. Braun*

Department of Chemistry, Humboldt-Universität zu Berlin, Brook-Taylor-Str. 2, 12489 Berlin, Germany

1. Materials and Methods **2**

2. Synthesis of Germylium Ions **2**

3. Stoichiometric C–F Bond Activation Reactions. **6**

4. General Procedures for Catalytic C–F Bond Activation Reactions **7**

5. X-Ray Diffraction Analysis **10**

6. Mass and NMR spectra **12**

7. References **29**

1. Materials and Methods

The samples were prepared in a glovebox and the reactions performed in JYoung NMR tubes using conventional Schlenk techniques. Benzene and hexane were dried over K-Solvona® and distilled before usage. *o*-Dichlorobenzene was stored over molecular sieve. All reagents were obtained from commercial sources and used as received.

NMR spectra were acquired at a Bruker DPX 300, Bruker AVANCE II 300 spectrometer at room temperature with tetramethylsilane as external standard. ^{1}H NMR and ^{13}C{^{1}H} NMR chemical shifts (δ) were referenced to residual *o*-$C_6D_4Cl_2$ (δ = 7.17 ppm and δ = 132.6 ppm, respectively). ^{19}F NMR spectra were calibrated externally to $CFCl_3$; ^{11}B NMR spectra to external $BF_3{\cdot}OEt_2$ and ^{31}P{^{1}H} NMR spectra to external 85% H_3PO_4. NMR assignments were supported by ^{1}H-^{1}H COSY, ^{1}H-^{13}C HMQC, ^{1}H-^{13}C HMBC, ^{1}H{^{19}F} and ^{1}H{^{31}P} experiments.

LIFDI-TOF-MS was measured with a Micromass Q-TOF-2 mass spectrometer, equipped with a Linden LIFDI source (Linden CMS GmbH). GC-MS was measured with an Agilent 6890N gas-phase chromatograph (Agilent 19091S-433 Hewlett-Packard) with an Agilent 5973 Network mass selective detector at 70 eV.

2. Synthesis of Germylium Ions

Synthesis of $[Et_3Ge][B(C_6F_5)_4]$ (1a)

$[Ph_3C][B(C_6F_5)_4]$ (50.0 mg, 54 μmol) and Et_3GeH (8.7 μL, 54 μmol) were dissolved in C_6D_6 (0.4 mL) and stirred for 5 min at room temperature. The colourless top phase was removed and the yellow bottom phase was washed with C_6D_6 (3 x 0.3 mL). For characterisation, the isolated yellow bottom phase was dissolved in *o*-$C_6D_4Cl_2$ (0.3 mL). A quantitative conversion of the starting materials based on the ^{1}H NMR spectrum yielded **1a**.

^{1}H NMR (300 MHz, *o*-$C_6D_4Cl_2$): δ = 1.23-1.13 (m, 6H, CH_2CH_3); 1.12-1.02 (m, 9H, CH_2CH_3) ppm.
^{13}C{^{1}H} NMR (75 MHz, *o*-$C_6D_4Cl_2$): δ = 149.0 (dm, $^1J_{C,F}$ = 240 Hz, CF); 138.8 (dm, $^1J_{C,F}$ = 243 Hz, CF); 137.0 (dm, $^1J_{C,F}$ = 244 Hz, CF); 14.5 (br s, CH_2); 7.9 (s, CH_3) ppm. The signal for the C_{ipso} of the anion could not be observed due to overlapping with the solvent signals.
^{19}F NMR (280 MHz, *o*-$C_6D_4Cl_2$): δ = -132.1 (m, 8F, CF); -162.5 (t, $^3J_{F,F}$ = 21 Hz, 4F, *p*-CF); -166.4 (m, 8F, CF) ppm.
^{11}B NMR (96 MHz, *o*-$C_6D_4Cl_2$): δ = -16.4 (s) ppm.
MS (LIFDI, *o*-$C_6H_4Cl_2$): m/z = 161 $[Et_3Ge]^+$; 133 $[Et_2GeH]^+$

Synthesis of $[Ph_3Ge][B(C_6F_5)_4]$ (1b)

$[Ph_3C][B(C_6F_5)_4]$ (50.0 mg, 54 μmol) and Ph_3GeH (16.5 mg, 54 μmol) were dissolved in C_6D_6 (0.4 mL) and stirred for 5 min at room temperature. The colourless top phase was removed and the yellow bottom phase was washed with C_6D_6 (3 x 0.3 mL). For characterisation, the isolated yellow bottom phase was dissolved in *o*-$C_6D_4Cl_2$ (0.3 mL) and the formation of **1b** was observed. Note that formation of $B(C_6F_5)_3$ was also detected (18% based on the ^{19}F NMR spectrum).

^{1}H NMR (300 MHz, *o*-$C_6D_4Cl_2$): δ = 7.82-7.68 (m, 9H, *Ph*); 7.68-7.56 (m, 6H, *Ph*) ppm.
^{13}C{^{1}H} NMR (75 MHz, *o*-$C_6D_4Cl_2$): δ = 149.0 (dm, $^1J_{C,F}$ = 239 Hz, CF); 138.8 (dm, $^1J_{C,F}$ = 244 Hz, CF); 136.9 (dm, $^1J_{C,F}$ = 248 Hz, CF); 135.7 (s, C_{ar}), 134.9 (s, C_{ipso}); 130.2 (s, C_{ar}) ppm. The signal for the C_{ipso} of the anion and the remaining signal of the phenyl ligands could not be observed due to overlapping with the solvent signals.
^{19}F NMR (280 MHz, *o*-$C_6D_4Cl_2$): δ = -131.3 (m, 8F, C*F*); -161.8 (t, $^3J_{F,F}$ = 21 Hz, 4F, *p*-C*F*); -165.7 (m, 8F, C*F*) ppm.
^{11}B NMR (96 MHz, *o*-$C_6D_4Cl_2$): δ = -16.3 (s) ppm.
MS (LIFDI, *o*-$C_6H_4Cl_2$): m/z = 305 $[Ph_3Ge]^+$.

Synthesis of [*n*Bu_3Ge][B(C_6F_5)$_4$] (1c)

$[Ph_3C][B(C_6F_5)_4]$ (50.0 mg, 54 μmol) and *n*Bu_3GeH (13.9 μL, 54 μmol) were dissolved in C_6D_6 (0.4 mL) and stirred for 5 min at room temperature. The colourless top phase was removed and the yellow bottom phase was washed with C_6D_6 (3 x 0.3 mL). For characterisation, the isolated yellow bottom phase was dissolved in *o*-$C_6D_4Cl_2$ (0.3 mL). The quantitative conversion of the starting materials based on the ^{1}H NMR spectrum yielded **1c**.

^{1}H NMR (300 MHz, *o*-$C_6D_4Cl_2$): δ = 1.57-1.47 (m, 12H, $CH_2CH_2CH_2CH_3$); 1.47-1.33 (m, 6H, $CH_2CH_2CH_2CH_3$); 1.02 (tm, $^3J_{H,H}$ = 7.0 Hz, 9H, CH_3) ppm.
^{13}C{^{1}H} NMR (75 MHz, *o*-$C_6D_4Cl_2$): δ = 148.9 (dm, $^1J_{C,F}$ = 244 Hz, CF); 138.7 (dm, $^1J_{C,F}$ = 243 Hz, CF); 136.8 (dm, $^1J_{C,F}$ = 245 Hz, CF); 25.9 and 25.6 (s, CH_2); 23.5 (br s, CH_2); 13.2 (s, CH_3) ppm. The signal for the C_{ipso} of the anion could not be observed due to overlapping with the solvent signals.
^{19}F NMR (280 MHz, *o*-$C_6D_4Cl_2$): δ = -131.7 (m, 8F, C*F*); -162.3 (t, $^3J_{F,F}$ = 21 Hz, 4F, *p*-C*F*); -166.1 (m, 8F, C*F*) ppm.
^{11}B NMR (96 MHz, *o*-$C_6D_4Cl_2$): δ = -16.2 (s) ppm.
MS (LIFDI, *o*-$C_6H_4Cl_2$): m/z = 245 [*n*$Bu_3Ge]^+$; 189 [*n*$Bu_2GeH]^+$.

Reaction of the germylium ion 1a with Et_3GeH: Formation of 2a

Reaction using 1 equivalent of Et_3GeH:

$[Ph_3C][B(C_6F_5)_4]$ (50.0 mg, 54 μmol) and Et_3GeH (9.8 μL, 59 μmol) were dissolved in C_6D_6 (0.4 mL) and stirred for 5 min at room temperature. The colourless top phase was removed and the yellow bottom phase was washed with C_6D_6 (3 x 0.3 mL). A second equivalent Et_3GeH (9.8 μL, 59 μmol) in C_6D_6 (0.3 mL) was added to the germylium ion **1a** and the bottom phase turned colourless. For characterisation, the isolated colourless bottom phase was dissolved in *o*-$C_6D_4Cl_2$ (0.3 mL). The quantitative conversion of **1a** based on the ^{1}H NMR spectrum yielded $[Et_3Ge\text{-}H\text{-}GeEt_3][B(C_6F_5)_4]$ (**2a**).

^{1}H NMR (300 MHz, *o*-$C_6D_4Cl_2$): δ = 2.08 (s br, 1H, Ge-*H*-Ge); 1.50-1.06 (m, 30H, CH_2CH_3) ppm.
^{13}C{^{1}H} NMR (75 MHz, *o*-$C_6D_4Cl_2$): δ = 149.0 (dm, $^1J_{C,F}$ = 242 Hz, CF); 138.8 (dm, $^1J_{C,F}$ = 245 Hz, CF); 136.9 (dm, $^1J_{C,F}$ = 244 Hz, CF); 9.7 (br s, CH_2); 9.0 (s br, CH_3) ppm. The signal of the C_{ipso} of the anion could not be observed due to overlapping with the solvent signals.
^{19}F NMR (280 MHz, *o*-$C_6D_4Cl_2$): δ = -131.8 (m, 8F, C*F*); -162.4 (t, $^3J_{F,F}$ = 21 Hz, 4F, *p*-C*F*); -166.2 (m, 8F, C*F*) ppm.
^{11}B NMR (96 MHz, *o*-$C_6D_4Cl_2$): δ = -16.1 (s) ppm.

Reaction using different equivalents of Et_3GeH:

Et_3GeH (5 µL, 32 µmol) was added to the solution of **2a** (32 µmol of trityl salt) in *o*-$C_6D_4Cl_2$ and the mixture stirred for 5 min at room temperature. ^1H NMR spectrum confirmed the consumption of the Et_3GeH. Then, more Et_3GeH (8 µL, 50 µmol) was added to the solution. NMR data confirmed the formation of $GeEt_4$ and traces of Et_2GeH_2.

Reaction of the germylium ion 1b with Ph_3GeH: Formation of 2b

$[Ph_3C][B(C_6F_5)_4]$ (50.0 mg, 54 µmol) and Ph_3GeH (16.5 mg, 54 µmol) were dissolved in C_6D_6 (0.4 mL) and stirred for 5 min at room temperature. The colourless top phase was removed and the yellow bottom phase was washed with C_6D_6 (3 x 0.3 mL). A second equivalent Ph_3GeH (16.5 mg, 54 µmol) in C_6D_6 (0.3 mL) was added to the germylium ion **1b** and the bottom phase turned colourless. For characterisation, the isolated colourless bottom phase corresponding to $[Ph_3Ge\text{-}H\text{-}GePh_3][B(C_6F_5)_4]$ (**2b**) was dissolved in *o*-$C_6D_4Cl_2$ (0.3 mL). Note that formation of $B(C_6F_5)_3$ was also observed.

^{1}H NMR (300 MHz, *o*-$C_6D_4Cl_2$): δ = 7.75-7.61 (m, 9H, H_{ar}); 7.61-7.51 (m, 6H, H_{ar}); 5.40 (s br, 1H, Ge-*H*-Ge) ppm.
^{13}C{^{1}H} NMR (75 MHz, *o*-$C_6D_4Cl_2$): δ = 148.9 (dm, $^1J_{C,F}$ = 240 Hz, CF); 138.6 (dm, $^1J_{C,F}$ = 243 Hz, CF); 136.8 (dm, $^1J_{C,F}$ = 242 Hz, CF); 135.5 (s, C_{ar}); 129.1 (s, C_{ar}) ppm. The signal for the C_{ipso} of the anion and the remaining signals of the phenyl ligands could not be observed due to overlapping with the solvent signals and with the signals corresponding to $B(C_6F_5)_3$.
^{19}F NMR (280 MHz, *o*-$C_6D_4Cl_2$): δ = -131.7 (m, 8F, C*F*); -162.2 (t, $^3J_{F,F}$ = 21 Hz, 4F, *p*-C*F*); -166.1 (m, 8F, C*F*) ppm.
^{11}B NMR (96 MHz, *o*-$C_6D_4Cl_2$): δ = -16.1 (s) ppm.

Reaction of the germylium ion 1c with *n*Bu_3GeH: Formation of 2c

$[Ph_3C][B(C_6F_5)_4]$ (50.0 mg, 54 µmol) and *n*Bu_3GeH (13.9 µL, 54 µmol) were dissolved in C_6D_6 (0.4 mL) and stirred for 5 min at room temperature. The colourless top phase was removed and the yellow bottom phase was washed with benzene (3 x 0.3 mL). A second equivalent *n*Bu_3GeH (13.9 µL, 54 µmol) in C_6D_6 (0.3 mL) was added to the germylium ion **1c** and the bottom phase turned colourless. For characterisation, the isolated colourless bottom phase was dissolved in *o*-$C_6D_4Cl_2$ (0.3 mL). The quantitative conversion of the starting materials based on the ^1H NMR spectrum yielded $[n\text{Bu}_3Ge\text{-}H\text{-}Ge\,n\text{Bu}_3][B(C_6F_5)_4]$ (**2c**).

^{1}H NMR (300 MHz, *o*-$C_6D_4Cl_2$): δ = 1.97 (s br, 1H, Ge-*H*-Ge); 1.75-1.42 (m, 36H, $CH_2CH_2CH_2CH_3$); 1.09 (tm, $^3J_{H,H}$ = 7.1 Hz, 18H, CH_3) ppm.
^{13}C{^{1}H} NMR (75 MHz, *o*-$C_6D_4Cl_2$): δ = 148.9 (dm, $^1J_{C,F}$ = 242 Hz, CF); 138.8 (dm, $^1J_{C,F}$ = 244 Hz, CF); 136.9 (dm, $^1J_{C,F}$ = 244 Hz, CF); 27.4, 26.1 and 18.1 (all s, CH_2); 13.6 (s, CH_3) ppm. The signal of the C_{ipso} of the anion could not be observed due to overlapping with the solvent signals.
^{19}F NMR (280 MHz, *o*-$C_6D_4Cl_2$): δ = -131.7 (m, 8F, C*F*); -162.5 (t, $^3J_{F,F}$ = 21 Hz, 4F, *p*-C*F*); -166.2 (m, 8F, C*F*) ppm.
^{11}B NMR (96 MHz, *o*-$C_6D_4Cl_2$): δ = -16.2 (s) ppm.

Synthesis of $[Et_3Ge\text{-}OH_2][B(C_6F_5)_4]$ (3)

Degassed H_2O (1 μl, 55 μmol) was added to a solution of $[Et_3Ge][B(C_6F_5)_4]$ (43 μmol) in *o*-$C_6D_4Cl_2$ (0.4 mL) and stirred for 5 min at room temperature. The quantitative conversion of the germylium ion yielded compound **3**. Crystals were obtained by adding hexane (0.4 mL) to a solution of **3** in *o*-$C_6H_4Cl_2$ (0.2 mL).

^{1}H NMR (300 MHz, *o*-$C_6D_4Cl_2$): δ = 5.1 (s, vbr, OH_2); 1.33-1.12 (m, CH_2CH_3) ppm.
^{19}F NMR (280 MHz, *o*-$C_6D_4Cl_2$): δ = -131.4 (m, 8F, C*F*); -162.0 (t, $^3J_{F,F}$ = 21 Hz, 4F, *p*-C*F*); -165.8 (m, 8F, C*F*) ppm.

Synthesis of $[Et_3Ge\text{-}PEt_3][B(C_6F_5)_4]$ (4a)

PEt_3 (5 μl, 35 μmol) was added to a solution of *in situ* synthesized $[Et_3Ge][B(C_6F_5)_4]$ (32 μmol of $[Ph_3C][B(C_6F_5)_4]$) in *o*-$C_6D_4Cl_2$ (0.4 mL) and the reaction mixture was stirred for 5 min at room temperature. Then, the excess of triethylphosphine was removed in vacuum, and the oily product **4a** obtained in a quantitative conversion (based on the ^{1}H and ^{31}P{^{1}H} NMR spectra) was dissolved in *o*-$C_6D_4Cl_2$ for characterisation.

^{31}P{^{1}H} NMR (121 MHz, *o*-$C_6D_4Cl_2$): δ = 1.94 (s, PEt_3) ppm.
^{1}H NMR (300 MHz, *o*-$C_6D_4Cl_2$): δ = 1.83 (dq, $^2J_{H,P}$ = 11.4 Hz, 6H, CH_2P); 1.31-1.01 (m, 24H, $GeCH_2CH_3$ + CH_3CH_2P) ppm.
^{13}C{^{1}H} NMR (75 MHz, *o*-$C_6D_4Cl_2$): δ = 148.9 (dm, $^1J_{C,F}$ = 238 Hz, CF); 138.8 (dm, $^1J_{C,F}$ = 246 Hz, CF); 136.9 (dm, $^1J_{C,F}$ = 245 Hz, CF); 18.5 (d, $^1J_{C,P}$ = 64 Hz, CH_2P); 8.3, 7.6, 6.8 (all s, CH_3CH_2Ge + CH_3CH_2P) ppm. The signal for the C_{ipso} of the anion could not be observed due to overlapping with the solvent signals.
^{19}F NMR (280 MHz, *o*-$C_6D_4Cl_2$): δ = -131.8 (m, 8F, C*F*); -162.3 (t, $^3J_{F,F}$ = 21 Hz, 4F, *p*-C*F*); -166.1 (m, 8F, C*F*) ppm.
^{11}B NMR (96 MHz, *o*-$C_6D_4Cl_2$): δ = -16.2 (s) ppm.

Synthesis of $[Et_3Ge\text{-}PPh_3][B(C_6F_5)_4]$ (4b)

PPh_3 (8.5 mg, 32 μmol) was added to a solution of *in situ* synthesized $[Et_3Ge][B(C_6F_5)_4]$ (32 μmol of $[Ph_3C][B(C_6F_5)_4]$) in *o*-$C_6D_4Cl_2$ (0.4 mL) and the reaction mixture was stirred for 5 min at room temperature. The quantitative conversion of the phosphine according to the ^{1}H and ^{31}P{^{1}H} NMR spectra yielded compound **4b**.

^{31}P{^{1}H} NMR (121 MHz, *o*-$C_6D_4Cl_2$): δ = 2.33 (s br, PPh_3) ppm.
^{1}H NMR (300 MHz, *o*-$C_6D_4Cl_2$): δ = 7.66 (pseudo q, $J_{H,H}$ = 7.6 Hz, 3H, *p*-$(C_6H_5)_3P$); 7.59 (tdm, $J_{H,H}$ = 7.6, $^4J_{H,P}$ = 2.3 Hz, 6H, *m*-$(C_6H_5)_3P$); 7.53 (dm, $^3J_{H,P}$ = 11.8 Hz, 3H, *o*-$(C_6H_5)_3P$); 7.48 (dm, $^3J_{H,P}$ = 11.7 Hz, 3H, *o*-$(C_6H_5)_3P$); 1.39-1.25 (m, 6H, CH_2CH_3); 1.22-1.10 (m, 9H, CH_2CH_3) ppm.
^{13}C{^{1}H} NMR (75 MHz, *o*-$C_6D_4Cl_2$): δ = 149.0 (dm, $^1J_{C,F}$ = 240 Hz, CF); 138.8 (dm, $^1J_{C,F}$ = 244 Hz, CF); 136.9 (dm, $^1J_{C,F}$ = 245 Hz, CF); 133.5 (d, $^2J_{C,P}$ = 13 Hz, *o*-$(C_6H_5)_3P$); 128.4 and 128.1 (s br, $(C_6H_5)_3P$); 8.7 (s, CH_3); 8.4 (br s, CH_2) ppm. The signasl for the C_{ipso} of the anion and the phosphine ligand could not be observed due to overlapping with the solvent signals.
^{19}F NMR (280 MHz, *o*-$C_6D_4Cl_2$): δ = -131.7 (m, 8F, C*F*); -162.4 (t, $^3J_{F,F}$ = 21 Hz, 4F, *p*-C*F*); -166.2 (m, 8F, C*F*) ppm.
^{11}B NMR (96 MHz, *o*-$C_6D_4Cl_2$): δ = -16.2 (s) ppm.

MS (LIFDI, *o*-$C_6H_4Cl_2$): m/z = 423 $[Et_3Ge\text{-}PPh_3]^+$

Reaction of 1a with Et_3GeF: Formation of 5a

$[Ph_3C][B(C_6F_5)]_4$ (35.0 mg, 38 µmol) and Et_3GeH (6.2 µL, 38 µmol) were dissolved in C_6D_6 (0.4 mL) and the solution was strirred for 5 min at room temperature. The colourless top phase was removed and the yellow bottom phase was washed with C_6D_6 (3 x 0.3 mL). An equivalent of Et_3GeF (5.9 µL, 38 µmol) was added to the germylium ion **1a** in C_6D_6. For characterisation, the isolated light yellow bottom phase was dissolved in *o*-$C_6D_4Cl_2$ (0.3 mL). The quantitative conversion of **1a** and the fluorogermane based on the ^1H NMR and $^{19}F\{^1H\}$ spectra yielded $[Et_3Ge\text{-}F\text{-}GeEt_3][B(C_6F_5)_4]$ (**5a**).

^{1}H NMR (300 MHz, *o*-$C_6D_4Cl_2$): δ = 1.37-1.04 (m, CH_2CH_3) ppm.
^{13}C{^{1}H} NMR (75 MHz, *o*-$C_6D_4Cl_2$): δ = 148.9 (dm, $^1J_{C,F}$ = 243 Hz, CF); 138.8 (dm, $^1J_{C,F}$ = 245 Hz, CF); 136.8 (dm, $^1J_{C,F}$ = 245 Hz, CF); 9.4 (s br, CH_2); 7.1 (s, CH_3) ppm. The signal of the C_{ipso} of the anion could not be observed due to overlapping with the solvent signals.
^{19}F NMR (280 MHz, *o*-$C_6D_4Cl_2$): δ = -131.7 (m, 8F, C*F*); -162.3 (t, $^3J_{F,F}$ = 20.7 Hz, 4F, *p*-C*F*); -166.2 (m, 8F, C*F*); -196.9 (s br, 1F, Ge-*F*-Ge) ppm.
^{11}B NMR (96 MHz, *o*-$C_6D_4Cl_2$): δ = -16.2 (s) ppm.

Reaction of 1b with Ph_3GeF: Formation of 5b

$[Ph_3C][B(C_6F_5)_4]$ (30.0 mg, 32 µmol) and Ph_3GeH (9.91 mg, 32 µmol) were dissolved in C_6D_6 (0.4 mL) and reaction mixture was strirred for 5 min at room temperature. The colourless top phase was removed and the yellow bottom phase was washed with C_6D_6 (3 x 0.3 mL). Then, Ph_3GeF (10.5 mg, 32 µmol) in C_6D_6 (0.3 mL) was added to germylium ion **1b**. For characterisation, the isolated light yellow bottom phase was dissolved in *o*-$C_6D_4Cl_2$ (0.3 mL). The quantitative conversion of **1b** and the fluorogermane based on the ^1H NMR and $^{19}F\{^1H\}$ spectra yielded $[Ph_3Ge\text{-}F\text{-}GePh_3][B(C_6F_5)_4]$ (**5b**).

^{1}H NMR (300 MHz, *o*-$C_6D_4Cl_2$): δ = 7.8-7.34 (m, H_{ar}) ppm.
^{13}C{^{1}H} NMR (125 MHz, *o*-$C_6D_4Cl_2$): δ = 149.1 (dm, $^1J_{C,F}$ = 242 Hz, CF); 138.9 (dm, $^1J_{C,F}$ = 244 Hz, CF); 136.7 (dm, $^1J_{C,F}$ = 248 Hz, CF); 134.7 (s, C_{ar}); 129.6 (s, C_{ar}); 128.6 (s, C_{ar}) ppm. Both signals for C_{ipso} could not be observed due to overlapping with the solvent's signals.
^{19}F NMR (280 MHz, *o*-$C_6D_4Cl_2$): δ = -131.6 (m, 8F, C*F*); -162.4 (t, $^3J_{F,F}$ = 21 Hz, 4F, *p*-C*F*); -166.1 (m, 8F, C*F*); -170.4 (s br, 1F, Ge-*F*-Ge) ppm.
^{11}B NMR (96 MHz, *o*-$C_6D_4Cl_2$): δ = -16.1 (s) ppm.

3. Stoichiometric C–F Bond Activation Reactions.

Formation of 5 and 1,2-dichloro-4-cyclohexylbenzene-d_3

In a JYoung NMR tube, $[R_3Ge][B(C_6F_5)_4]$ (R= Et (**1a**), ^{n}Bu (**1c**)) (32 µmol) or $[R_3Ge\text{-}H\text{-}GeR_3][B(C_6F_5)_4]$ (R= Et (**3a**), *n*Bu (**3c**)) (32 µmol) was dissolved in *o*-$C_6D_4Cl_2$ (0.4 mL). Then fluorocyclohexane (3.6 µL, 32 µmol) was added. After 5 minutes, full conversion of the fluorocyclohexane and formation of 1,2-dichloro-4-cyclohexylbenzene-d_3 together with the formation of species such as $[R_3Ge\text{-}F\text{-}GeR_3][B(C_6F_5)_4]$ (R= Et (**5a**), *n*Bu (**5c**)) were observed. The Friedel Craft product was identify based on the non-deuterated derivative described in the literature.[1]

NMR data for R = *n*Bu (**5c**):

^{1}H NMR (300 MHz, *o*-$C_6D_4Cl_2$): δ = 1.70-1.43 (m, 36H, $CH_2CH_2CH_2CH_3$); 1.14-1.04 (m, 18H, CH_3) ppm.

^{13}C{^{1}H} NMR (75 MHz, *o*-$C_6D_4Cl_2$): δ = 148.9 (dm, $^1J_{C,F}$ = 243 Hz, CF); 138.8 (dm, $^1J_{C,F}$ = 244 Hz, CF); 136.9 (dm, $^1J_{C,F}$ = 244 Hz, CF); 26.1, 25.6 and 18.7 (all s, CH_2); 13.6 (s, CH_3) ppm. The signal of the C_{ipso} of the anion could not be observed due to overlapping with the solvent's signals.

^{19}F NMR (280 MHz, *o*-$C_6D_4Cl_2$): δ = -131.7 (m, 8F, C*F*); -162.4 (t, $^3J_{F,F}$ = 20.7 Hz, 4F, *p*-C*F*); -166.2 (m, 8F, C*F*); -201.6 (s br, Ge-*F*-Ge) ppm.

^{11}B NMR (96 MHz, *o*-$C_6D_4Cl_2$): δ = -16.2 (s) ppm.

4. General Procedures for Catalytic C–F Bond Activation Reactions

Activation of fluorocyclohexane

In a JYoung NMR tube, $[Ph_3C][B(C_6F_5)_4]$ (9.2 mg, 0.01 mmol) was dissolved in *o*-$C_6D_4Cl_2$ (0.4 mL). Then, R_3GeH (R = Et, ^{n}Bu) (0.2 or 0.4 mmol) and fluorocyclohexane (0.1 or 0.2 mmol) were added. H_2 evolution was observed. The reactions were performed either at room temperature or under heating (Table S1). The reaction progress was monitored by ^{1}H and ^{19}F NMR spectroscopy. For the reaction without solvent, same procedure was used and after the reaction time C_6D_6 was added in order to measure the NMR. The products were identified by their characteristic signals in the ^{1}H or ^{19}F NMR spectra (Tables S3 and S4).

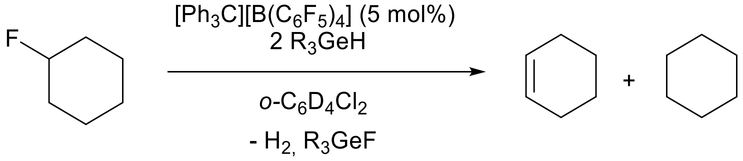

Table S1. C-F activation of fluorocyclohexane by germylium ions.

R	T (°C)	Time	Conversion (%)^a	Products ratio
Et	rt	30 min	100	7:1
Et^b	rt	5 h	99	12:1
Et^c	100	1 d	100	10:1
Et^d	rt	30 min	100	5:1
*n*Bu	rt	4 d	23	1:0
*n*Bu	65	2 h	100	3:1

a) Based on consumption of fluorocyclohexane by integration of the ^{19}F NMR spectra. b) 2.5 mol% of catalyst. c) Compound **4b** as catalytic precursor. d) Reaction in neat conditions

Activation of other fluorinated substrates

In a JYoung NMR tube, $[Ph_3C][B(C_6F_5)_4]$ (9.2 mg, 0.01 mmol) was dissolved in *o*-$C_6D_4Cl_2$ (0.4 mL). Then, Et_3GeH (0.2 or 0.4 mmol) and the fluorinated substrate (0.1 or 0.2 mmol) were added. H_2 evolution was observed. The Reactions took place at room temperature or at 65°C (Table S2). The reaction progress was monitored by ^{1}H and ^{19}F NMR spectroscopy. The products were identified by characteristic signals in the ^{1}H or ^{19}F NMR spectra (Tables S3 and S4).

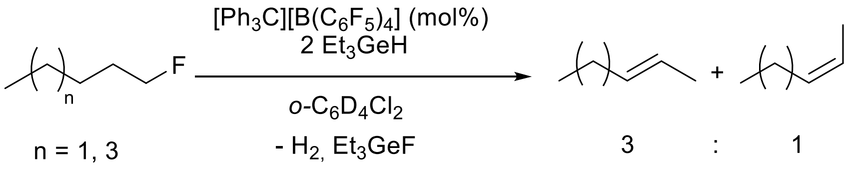

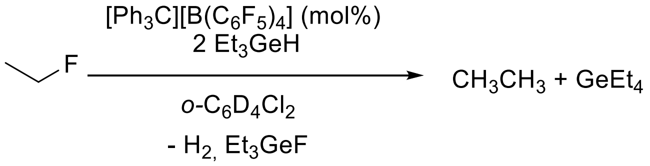

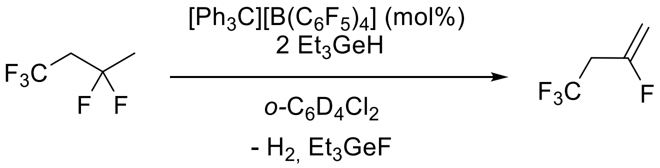

Table S2. Dehydrofluorination reaction by germylium ions

Substrate	Mol%	T (°C)	Time	Conversion (%)[a]
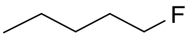	5	rt	1 d[b]	62
	10	rt	1 d[c]	73
	5	65	6 h 30 min	99
	10	65	3 h	100
	10[d]	65	4 h	99
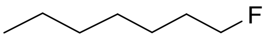	10	65	5 h	100
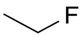	10	65	1 w	99
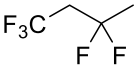	10	65	3d	5

a) Based on consumption of fluorocyclohexane by integration of the ^{19}F NMR spectra. b) 3d, 66% conversion. c) 3d, 77% conversion. d) nBu_3GeH used as hydrogen source.

Table S3 Selected NMR resonances of substrates in *ortho*-dichlorobenzene

Substrate	δ (^{1}H NMR) [ppm]	δ (^{19}F NMR) [ppm]
Et_3GeH	3.96 (hept, $^{3}J_{H,H}$ = 2.8 Hz, 1H, HGe); 1.26 (t, $^{3}J_{H,H}$ = 7.9 Hz, 9H, CH_3); 0.99 (qd, $^{3}J_{H,H}$ = 7.9, $^{3}J_{H,H}$ = 2.8 Hz, 6H, CH_2)	-
Et_3GeF	1.29-1.24 (m, 9H, CH_3); 1.23-1.15 (m, 6H, CH_2)	-211.5 (hept br, $^{3}J_{F,H}$ = 5 Hz)
nBu_3GeH	4.04 (hept, $^{3}J_{H,H}$ = 3.0 Hz, 1H, HGe); 1.69-1.47 (m, 12H, $Ge(CH_2)_2$); 1.11 (t, $^{3}J_{H,H}$ = 7.1 Hz, 9H, CH_3); 1.07-0.99 (m, 6H, CH_2CH_3)	-
Ph_3GeH	7.77-7.68 (m, 6H, H_{ar}); 7.57-7.46 (m, 9H, H_{ar}); 5.94 (s, 1H, HGe)	-
Ph_3GeF	7.89-7.81 (m, 6H, H_{ar}); 7.64-7.52 (m, 9H, H_{ar})	-200.9 (s)
Fluoropentane	4.51 (dt, $^{2}J_{H,F}$ = 47.6, $^{3}J_{H,H}$ = 6.2 Hz, 2H, CH_2F); 1.76 (dm, $^{3}J_{H,F}$ = 24.4 Hz, 2H, CH_2CH_2F); 1.51-1.37 (m, 2H, CH_2CH_3); 1.06-1.00 (m, 3H, CH_2CH_3)	-216.7 (hept, $^{2}J_{F,H}$ = 24 Hz)
Fluorocyclohexane	4.66 (dtt, $^{2}J_{H,F}$ = 48.9, $^{3}J_{H,H}$ = 7.8, $^{3}J_{H,H}$ = 3.9 Hz, 1H, CHF); 2.02-1.88 (m, 2H, CH_2); 1.88-1.79 (m, 2H, CH_2); 1.79-1.66 (m, 2H, CH_2); 1.60-1.48 (m, 2H, CH_2); 1.48-1.34 (m, 2H, CH_2)	-172.2 (s br)
Fluoroethane	4.57 (dq, $^{2}J_{H,F}$ = 47.0, $^{3}J_{H,H}$ = 7.0 Hz, 2H, CH_2F); 1.42 (dt, $^{2}J_{H,F}$ = 26.0, $^{3}J_{H,H}$ = 7.0 Hz, 3H, CH_3)	-209.9 (tq, $^{2}J_{F,H}$ = 70, $^{2}J_{F,H}$ = 26 Hz)
1,1,1,3,3-Pentafluorobutane	2.76 (tq, $^{3}J_{H,F}$ = 13.6, $^{3}J_{H,F}$ = 10.3 Hz, 2H, CH_2); 1.78 (t, $^{3}J_{H,F}$ = 18.7, 3H, CH_3)	-61.8 (pseudo pent, $^{3}J_{F,H}$ ≈ $^{4}J_{F,F}$ = 10 Hz, CF_3); - 86.8 (m, CF_2)

Table S4 Selected NMR resonances of products in *ortho*-dichlorobenzene

Product	δ (^{1}H NMR) [ppm]	δ(^{19}F NMR) [ppm]
Z-2-pentene	5.60-5.50 (m, 2H, CH=CH); 1.75 (dm, $^{3}J_{H,H}$ = 5.2 Hz, H_3C-C=C)	
E-2-pentene	5.66-5.48 (m, 2H, CH=CH); 1.80 (dm, $^{3}J_{H,H}$ = 5.9 Hz, H_3C-C=C)	
cyclohexene	5.86-5.68 (m, 2H, CH=CH); 2.20-2.06 (m, 2H, CH_2)	
cyclohexane	1.59 (s, CH_2)	
H_2	4.75 (s)	-
nBu_3GeF	n.d.	-205.2 (m)
Z-2-heptene	5.74-5.46 (m, 2H, CH=CH); 1.78 (dm, $^{3}J_{H,H}$ = 4.5 Hz, H_3C-C=C)	
E-2-heptene	5.74-5.46 (m, 2H, CH=CH); 1.82 (dm, $^{3}J_{H,H}$ = 4.8 Hz, H_3C-C=C)	
Ethane	1.36 (s)	
2,4,4,4-tetrafluoro-1-butene	4.94 (dd, $^{3}J_{H,F}$ = 16.0, $^{3}J_{H,H}$ = 3.6 Hz, 1H, =CH_2); 4.62 (dd, $^{3}J_{H,F}$ = 47.2, $^{3}J_{H,H}$ = 3.6 Hz, 1H, =CH_2)	-64.8 (td, $^{3}J_{F,H}$ = 10, $^{4}J_{F,F}$ = 7 Hz, CF_3); -94.5 (dtq, $^{3}J_{F,H}$ = 47, $^{3}J_{F,H}$ = 16, $^{4}J_{F,F}$ = 7 Hz, CF)

5. X-Ray Diffraction Analysis

For the structure determination, the data collection was performed with a BRUKER D8 VENTURE area detector using Mo-K_α radiation (λ = 0.71073 Å). Multiscan absorption corrections implemented in SADABS[2] were applied to the data. The structures were solved by intrinsic phasing method (SHELXT-2013)[3] and refined by full-matrix least square procedures based on F2 with all measured reflections (SHELXL-2013), with anisotropic temperature factors for all non-hydrogen atoms. All carbon bound hydrogen atoms were added geometrically and refined by using a riding model. Crystallographic data (excluding structure factors) for the structures in this paper have been deposited with the Cambridge Crystallographic Data Centre, CCDC 1983059.

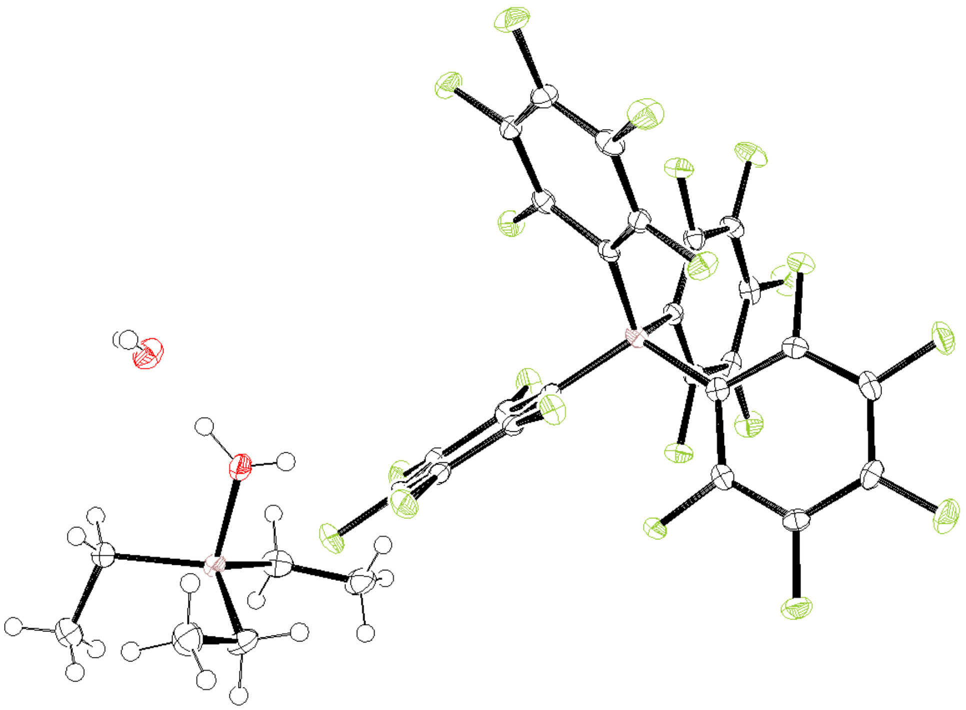

Figure S1. ORTEP representation of $[Et_3Ge-OH_2][B(C_6F_5)_4]\ H_2O$ (**3·H₂O**).

Table 3. Cristal data and structure refinement for compound **3·H₂O**.

Empirical formula	$C_{30}H_{19}BF_{20}GeO_2$	Crystal size	0.60 x 0.355 x 0.24 mm^3
Formula weight	874.85	θ range for data collection	2.165° to 25.082°.
Temperature	100(2) K	Index ranges	-17<=h<=17, -20<=k<=20, -29<=l<=28
Wavelength	0.71073 Å	Reflections collected	75256
Crystal system	Orthorhombic	Independent reflections	5570 [R(int) = 0.0323]
Space group	Pbca	Completeness to θ = 25.082°	99.8 %
Unit cell dimensions	a = 14.3032(13) Å	Absorption correction	Semi-empirical from equivalents
	b = 17.5925(15) Å	Max. and min. transmission	0.7452 and 0.5653
	c = 24.968(2) Å	Refinement method	Full-matrix least-squares on F^2
Volume	6282.8(10) Å^3	Data/ restraints / parameters	5570 / 1 / 504
Z	8	Goodness-of-fit on F^2	1.017
Density (calculated)	1.850 mg/m^3	Final R indices [I>2sigma(I)]	R1 = 0.0276, wR2 = 0.1051
Absorption coefficient	1.125 mm^{-1}	R indices (all data)	R1 = 0.0312, wR2 = 0.1112
F(000)	3456	Largest diff. peak and hole	0.359 and -0.711 e. Å^{-3}

6. Mass and NMR spectra

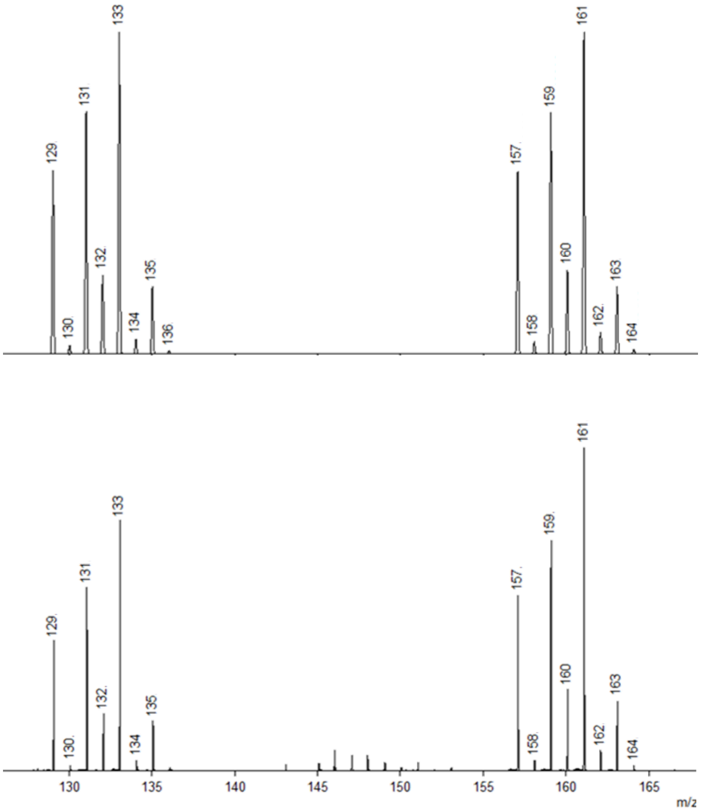

Figure S2. Experimental (bottom) and simulated (up) mass spectrum of $[Et_3Ge]^+$.

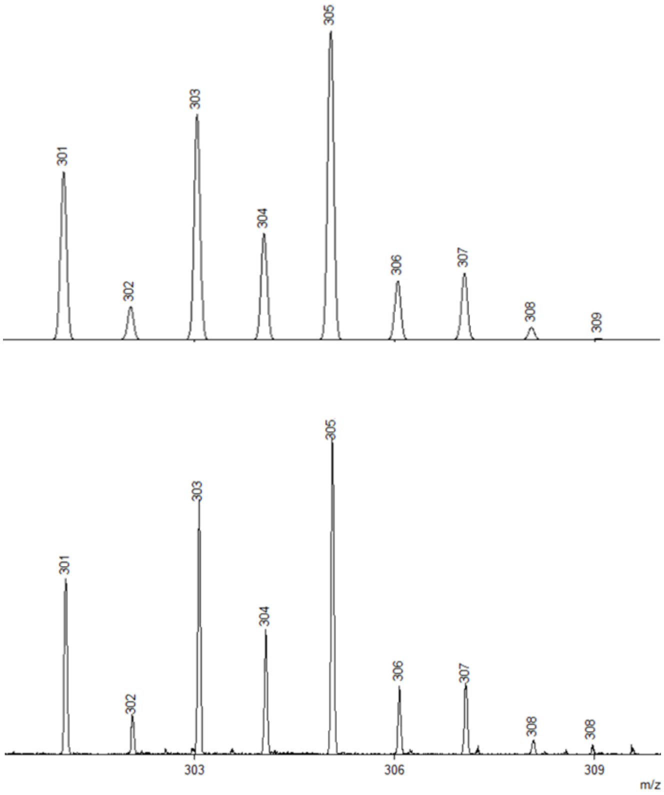

Figure S3. Experimental (bottom) and simulated (up) mass spectrum of $[Ph_3Ge]^+$.

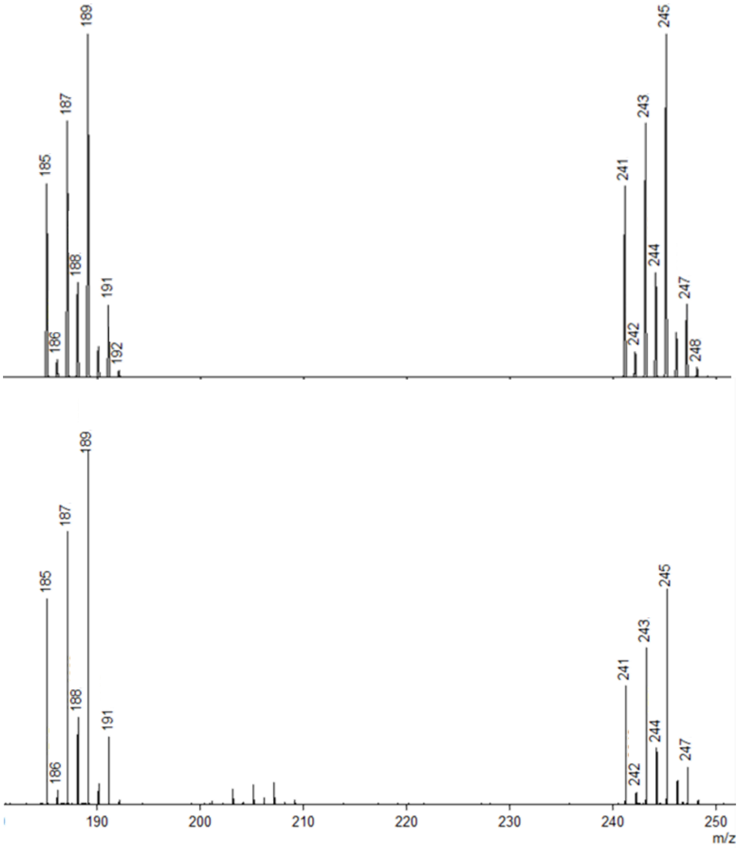

Figure S4. Experimental (bottom) and simulated (up) mass spectrum of [nBu$_3$Ge]$^+$.

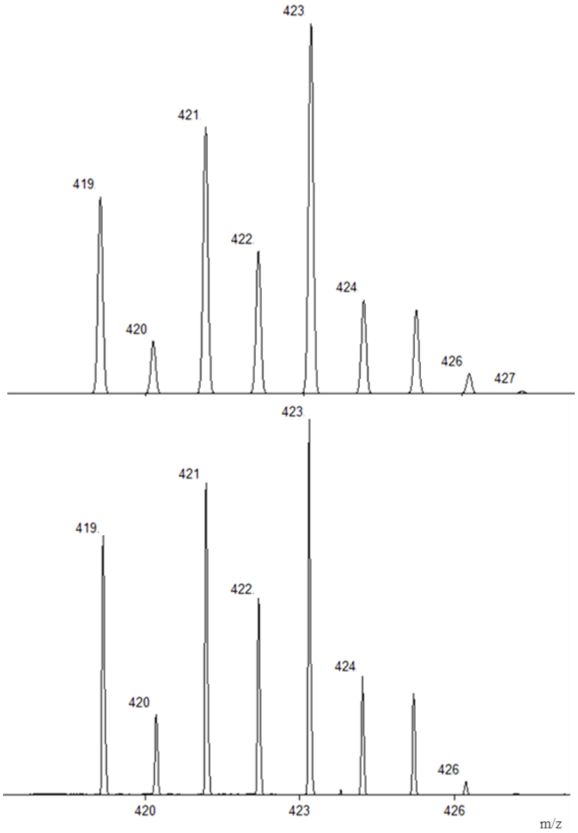

Figure S5. Experimental (bottom) and simulated (up) mass spectrum of [Et$_3$Ge-PPh$_3$]$^+$.

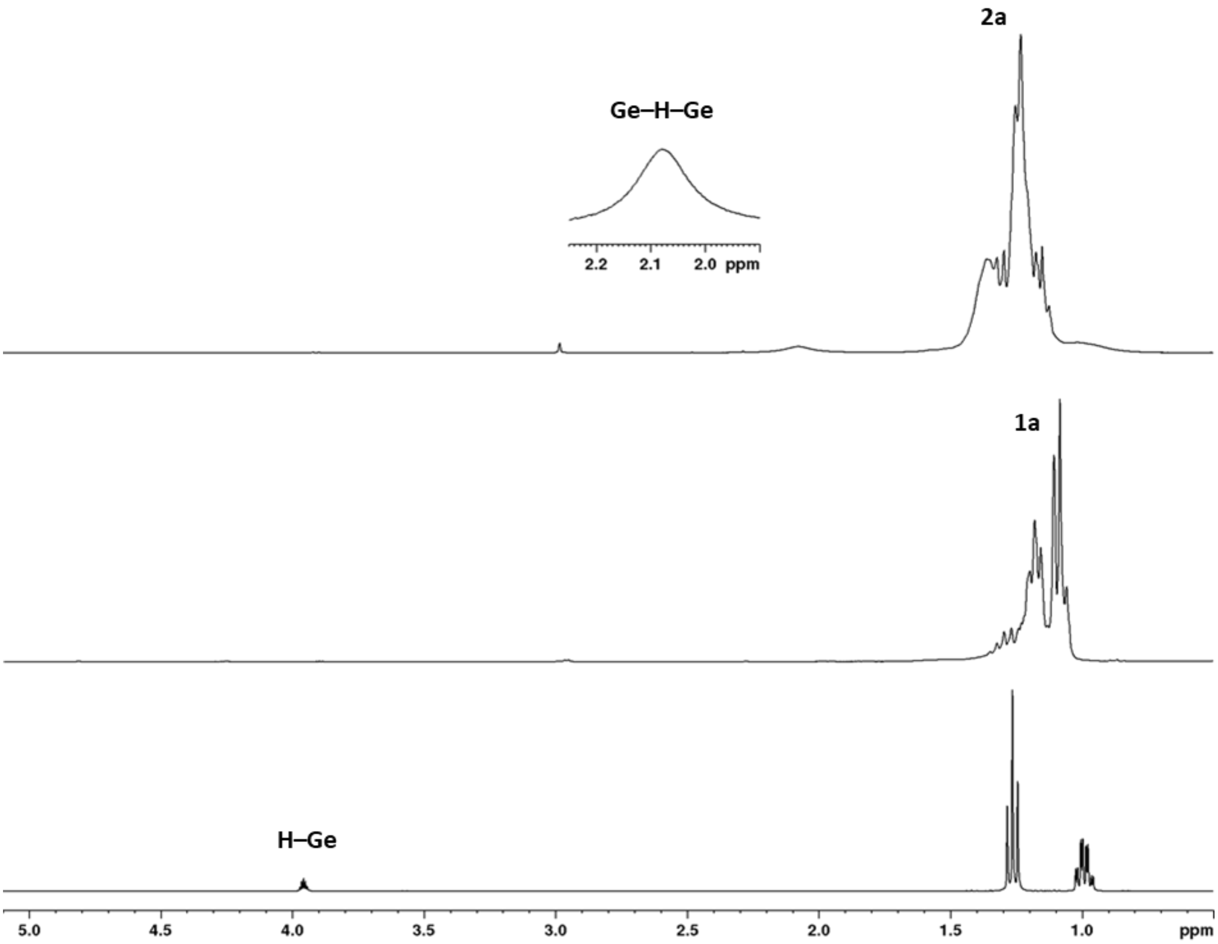

Figure S6. Section of the ^{1}H NMR spectra of Et_3GeH (bottom), $[Et_3Ge][B(C_6F_5)_4]$ (**1a**, middle) and $[Et_3GeHGeEt_3][B(C_6F_5)_4]$ (**2a**, top) in *o*-dichlorobenzene-d$_4$.

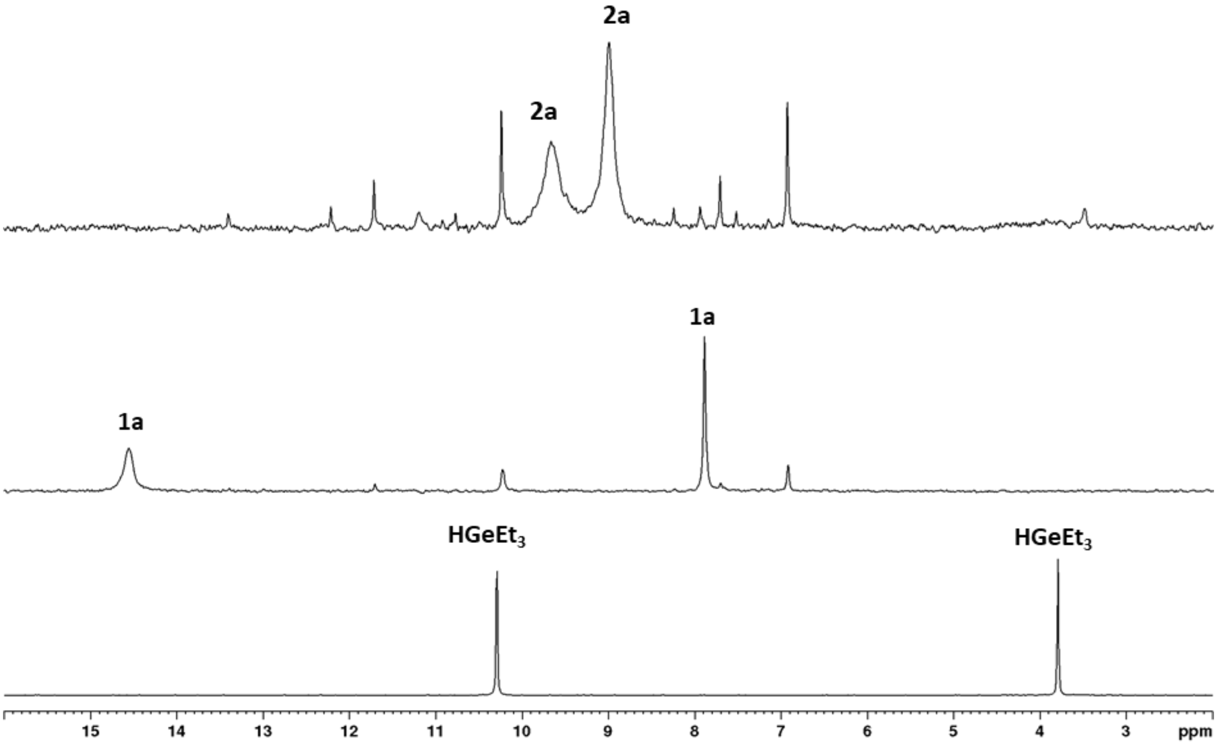

Figure S7. Section of the $^{13}C\{^1H\}$ NMR spectra of Et_3GeH (bottom), $[Et_3Ge][B(C_6F_5)_4]$ (**1a**, middle) and $[Et_3GeHGeEt_3][B(C_6F_5)_4]$ (**2a**, top) in *o*-dichlorobenzene-d4.

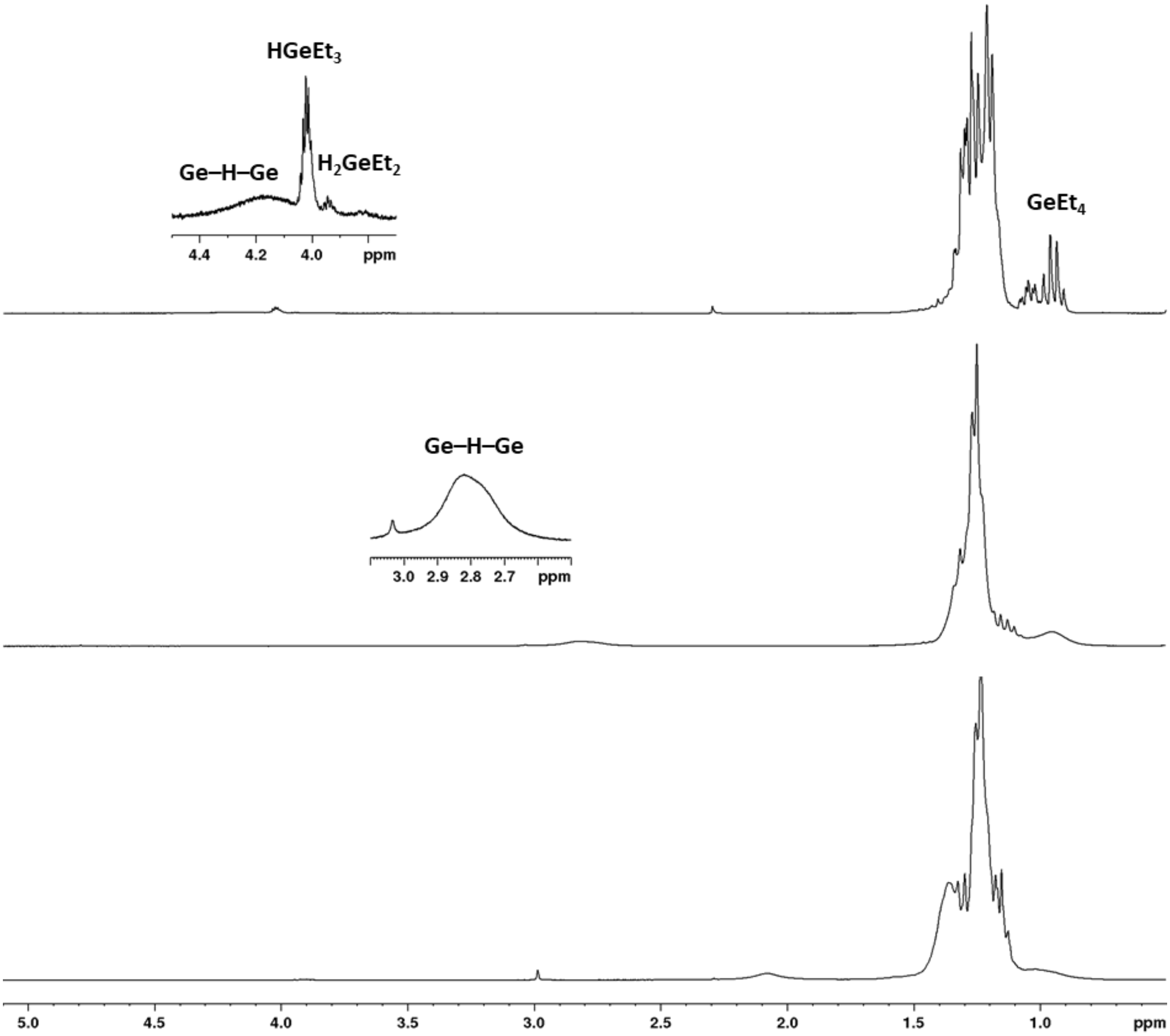

Figure S8. Section of the ^{1}H NMR spectra of [Et$_3$GeHGeEt$_3$][B(C$_6$F$_5$)$_4$] (**2a**, bottom) and after addition of 1 equivalent (middle) or excess (top) of HGeEt$_3$ in *o*-dichlorobenzene-d$_4$.

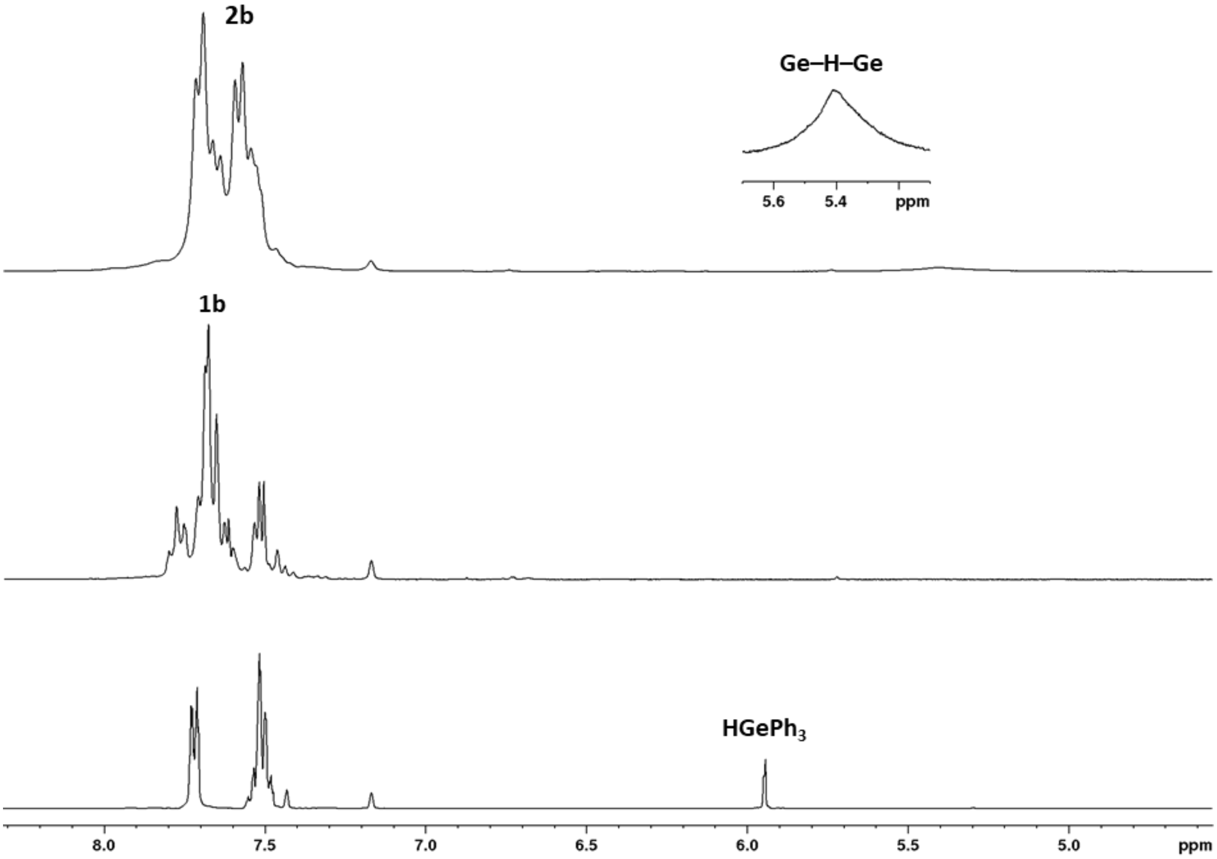

Figure S9. Section of the ^{1}H NMR spectra of Ph$_3$GeH (bottom), [Ph$_3$Ge][B(C$_6$F$_5$)$_4$] (**1b**, middle) and [Ph$_3$GeHGePh$_3$][B(C$_6$F$_5$)$_4$] (**2b**, top) in *o*-dichlorobenzene-d$_4$.

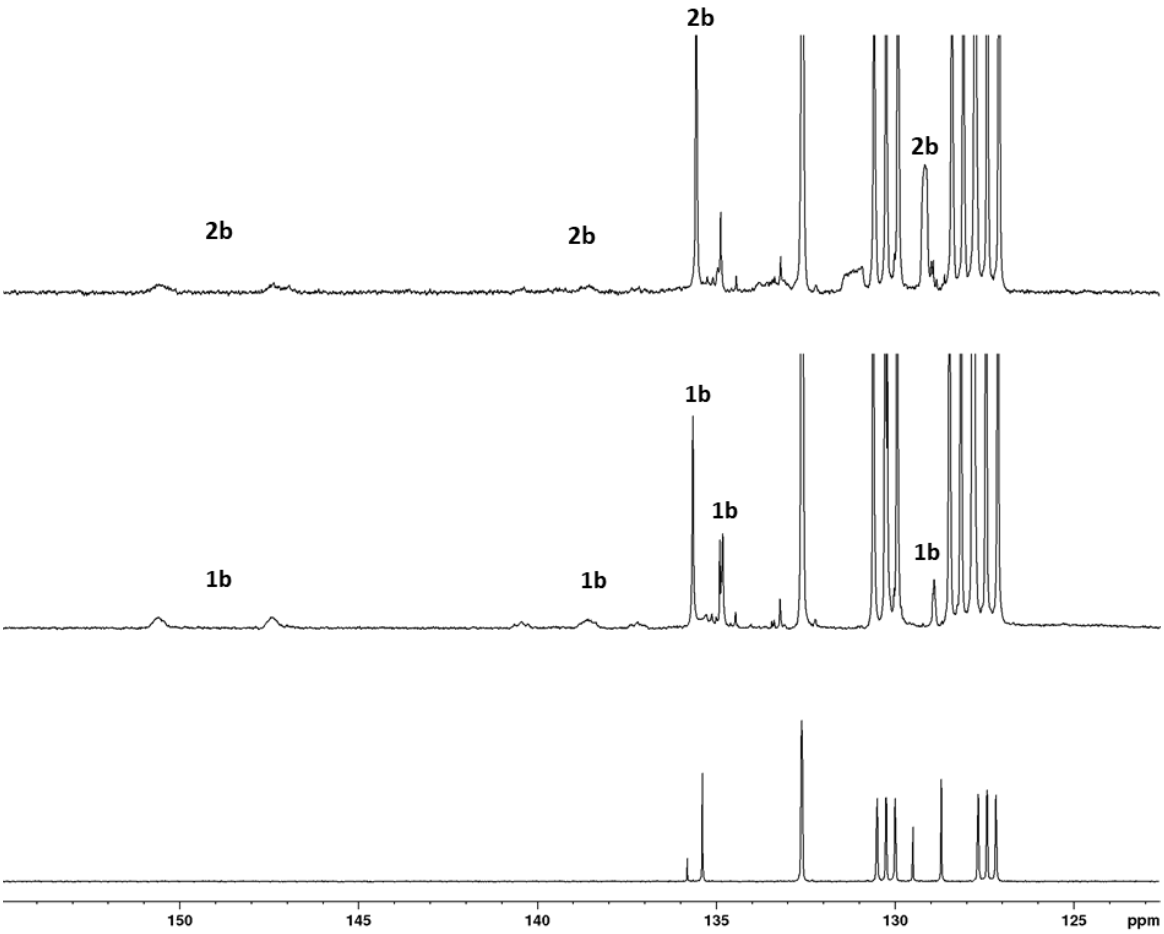

Figure S10. $^{13}C\{^1H\}$ NMR spectra of Ph_3GeH (bottom), $[Ph_3Ge][B(C_6F_5)_4]$ (**1b**, middle) and $[Ph_3GeHGePh_3][B(C_6F_5)_4]$ (**2b**, top) in *o*-dichlorobenzene-d$_4$. Note that C_6D_6 was not completely removed.

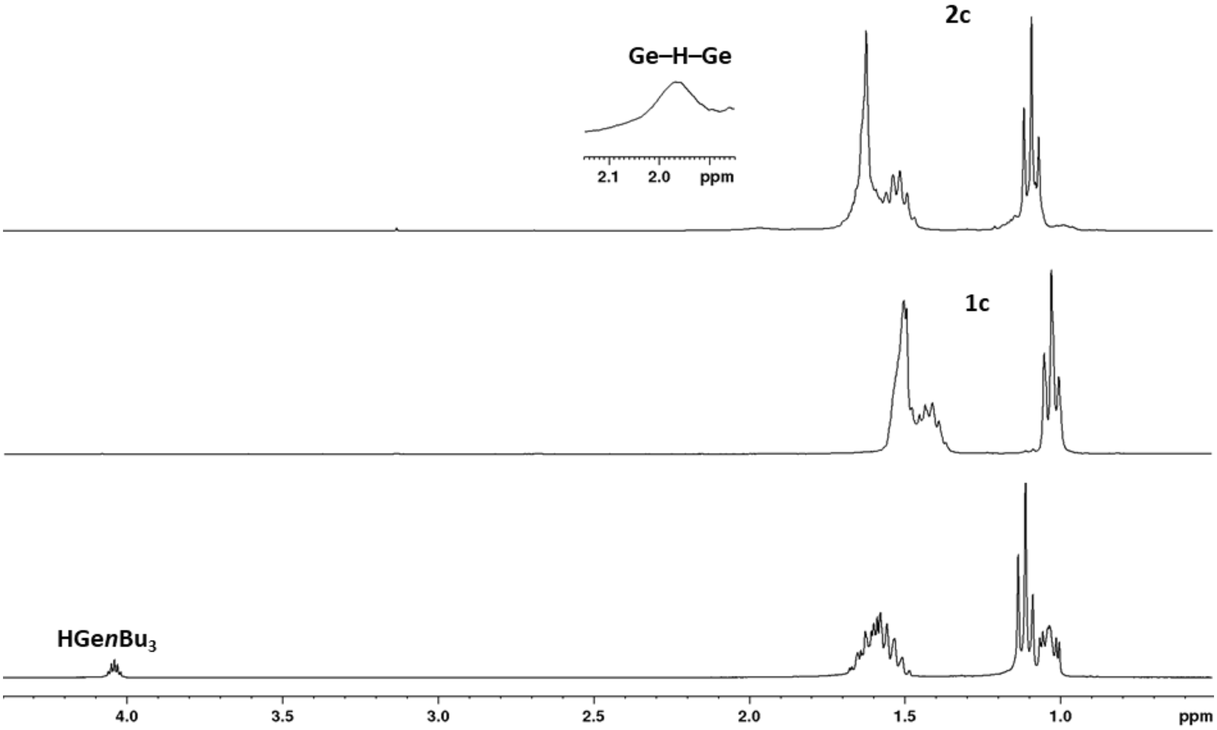

Figure S11. Section of the ^1H NMR spectra of *n*Bu_3GeH (bottom), [*n*$Bu_3Ge][B(C_6F_5)_4]$ (**1c**, middle) and [*n*Bu_3GeHGe*n*$Bu_3][B(C_6F_5)_4]$ (**2c**, top) in *o*-dichlorobenzene-d$_4$.

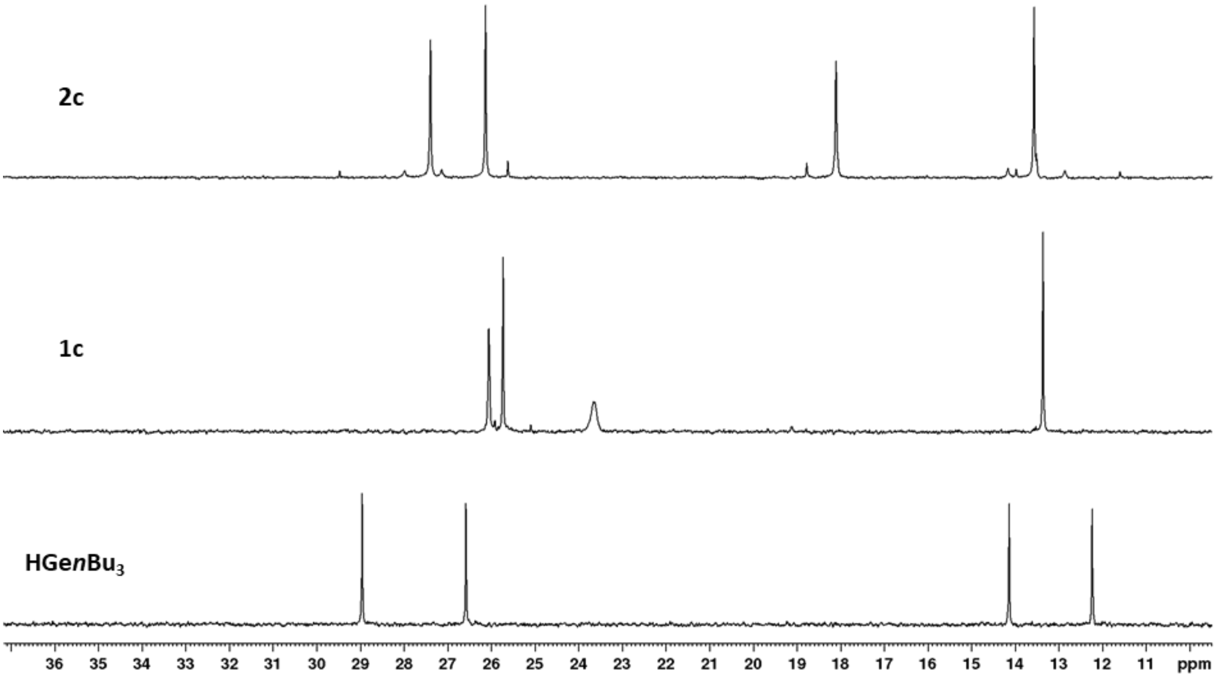

Figure S12. Section of the $^{13}C\{^1H\}$ NMR spectra of nBu_3GeH (bottom), $[nBu_3Ge][B(C_6F_5)_4]$ (**1c**, middle) and $[nBu_3GeHGenBu_3][B(C_6F_5)_4]$ (**2c**, top) in *o*-dichlorobenzene-d₄.

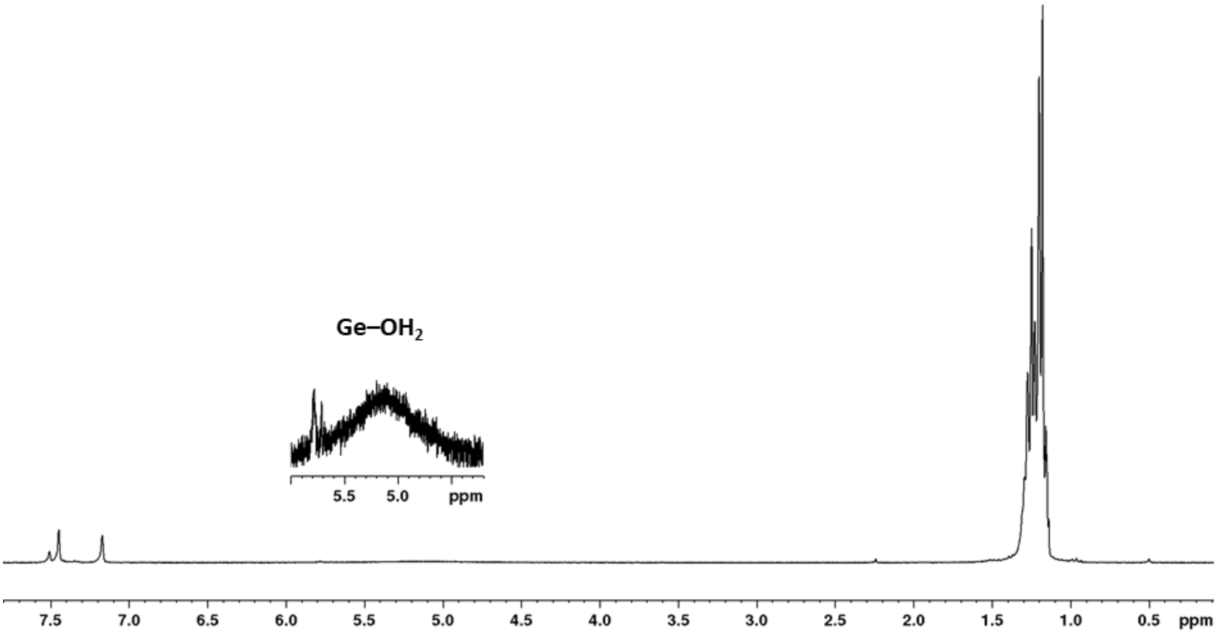

Figure S13. ^1H NMR spectrum of $[Et_3Ge\text{-}OH_2][B(C_6F_5)_4]$ (**3**) in *o*-dichlorobenzene-d₄. Note that C_6D_6 was not completely removed.

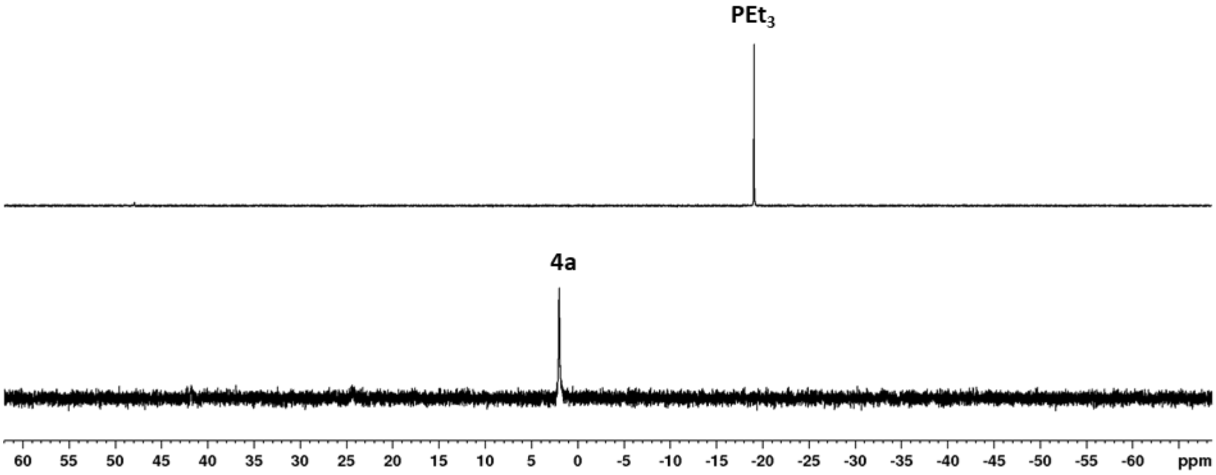

Figure S14. $^{31}P\{^1H\}$ NMR spectra of $[Et_3Ge\text{-}PEt_3][B(C_6F_5)_4]$ (**4a**, bottom) and PEt_3 (top) in *o*-dichlorobenzene-d$_4$.

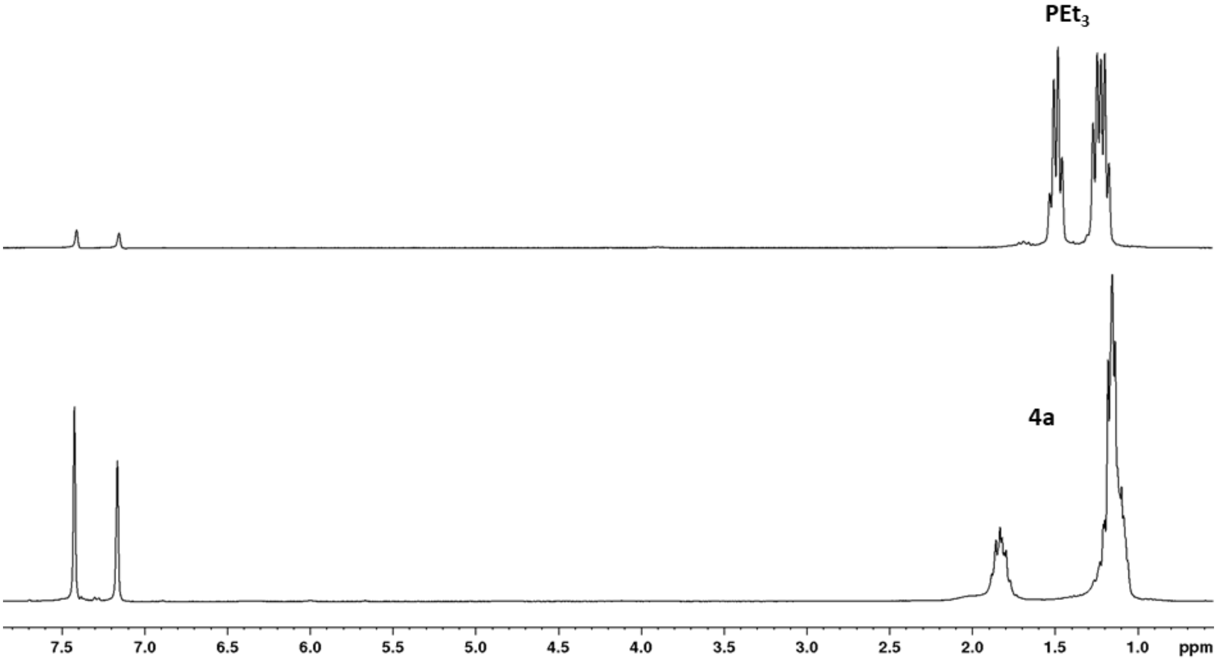

Figure S15. ^1H NMR spectra of $[Et_3Ge\text{-}PEt_3][B(C_6F_5)_4]$ (**4a**, bottom) and free PEt_3 (top) in *o*-dichlorobenzene-d$_4$.

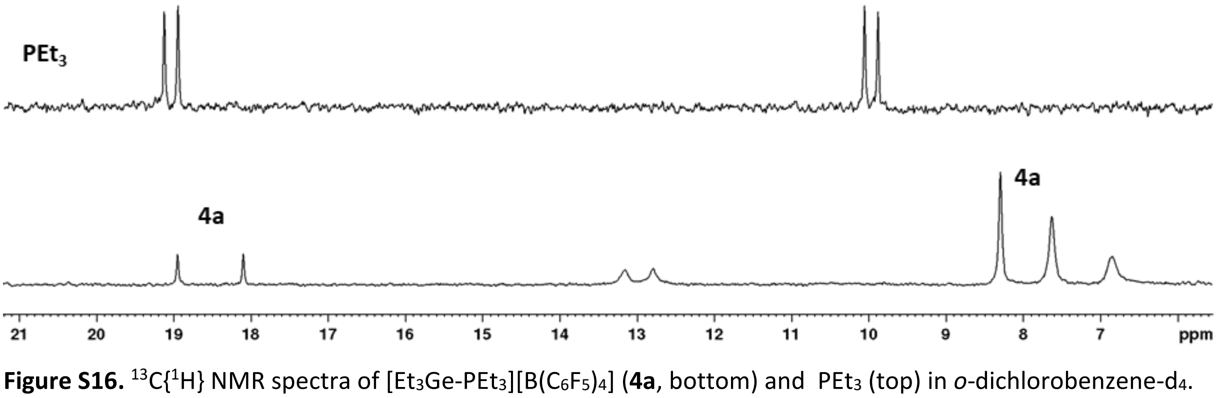

Figure S16. $^{13}C\{^1H\}$ NMR spectra of $[Et_3Ge\text{-}PEt_3][B(C_6F_5)_4]$ (**4a**, bottom) and PEt_3 (top) in *o*-dichlorobenzene-d$_4$.

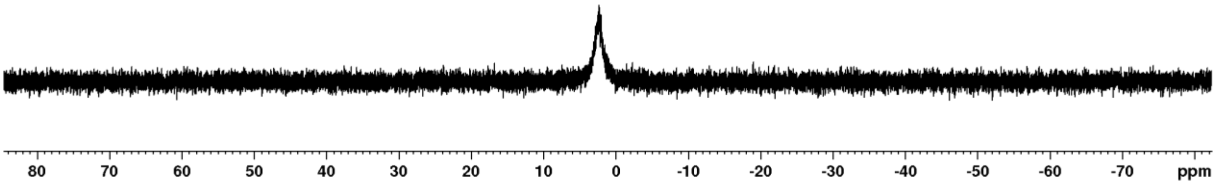

Figure S17. $^{31}P\{^1H\}$ NMR spectrum of $[Et_3Ge\text{-}PPh_3][B(C_6F_5)_4]$ (**4b**) in *o*-dichlorobenzene-d_4.

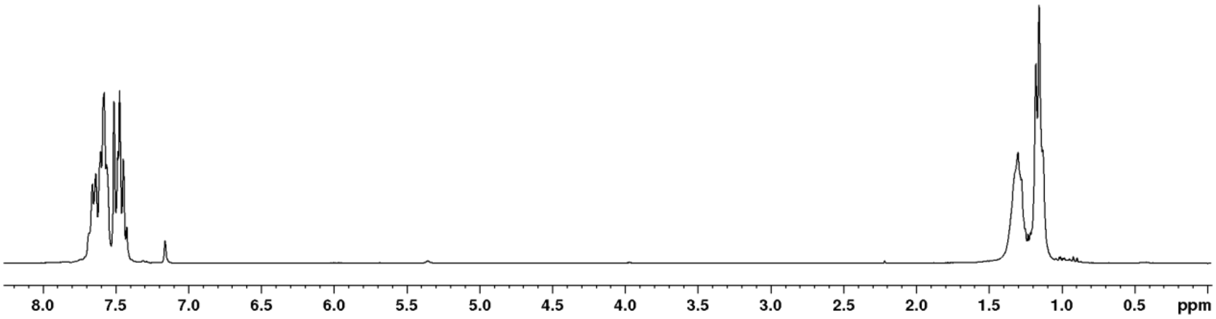

Figure S18. ^1H NMR spectrum of $[Et_3Ge\text{-}PPh_3][B(C_6F_5)_4]$ (**4b**) in *o*-dichlorobenzene-d_4. Note that C_6D_6 was not completely removed.

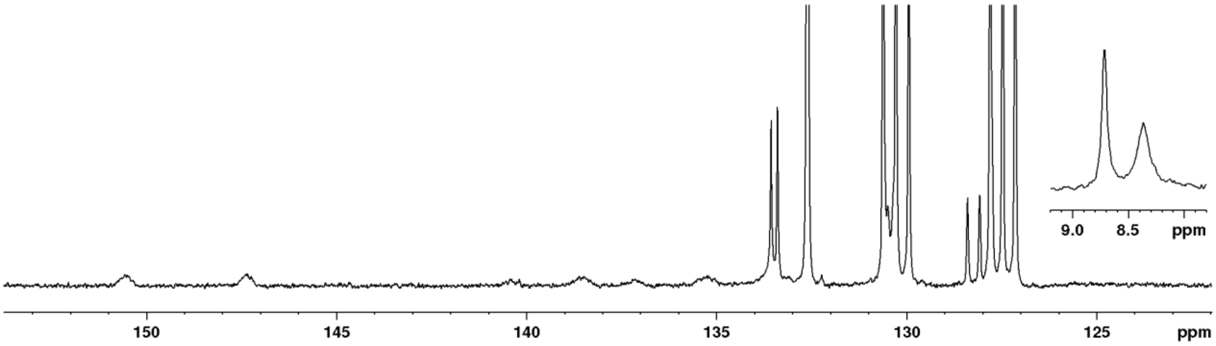

Figure S19. $^{13}C\{^1H\}$ NMR spectrum of $[Et_3Ge\text{-}PPh_3][B(C_6F_5)_4]$ (**4b**) in *o*-dichlorobenzene-d_4. Note that C_6D_6 was not completely removed.

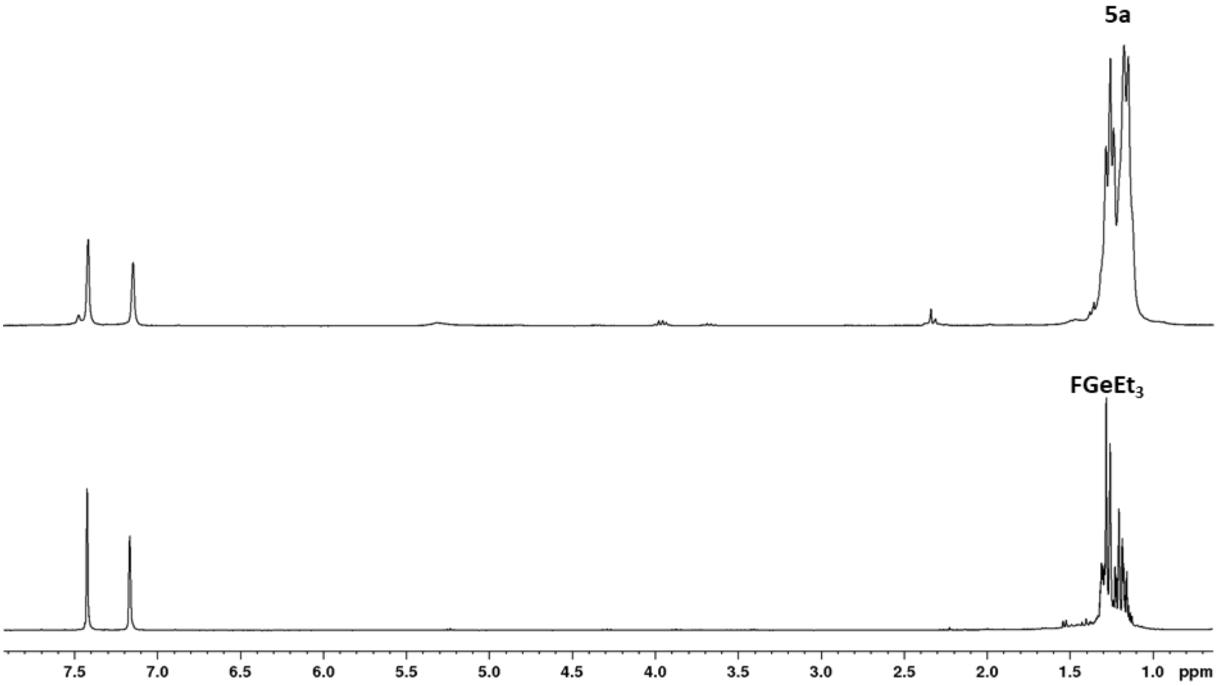

Figure S20. ^{1}H NMR spectra of Et_3GeF (bottom) and $[Et_3GeFGeEt_3][B(C_6F_5)_4]$ (**5a**, top) in *o*-dichlorobenzene-d$_4$. Note that C_6D_6 was not completely removed.

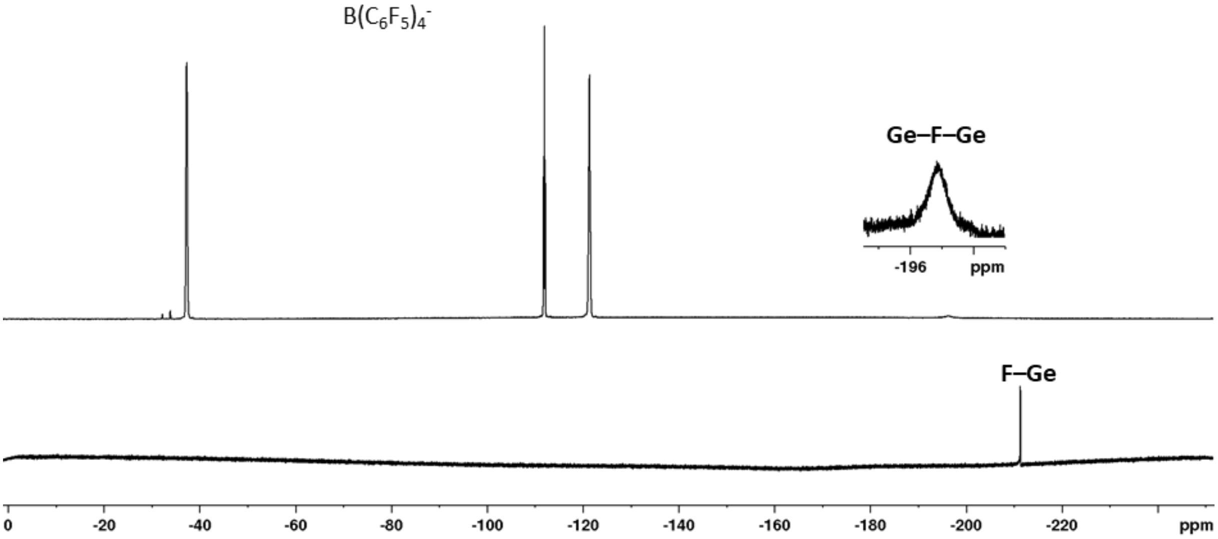

Figure S21. ^{19}F NMR spectra of Et_3GeF (bottom) and $[Et_3GeFGeEt_3][B(C_6F_5)_4]$ (**5a**, top) in *o*-dichlorobenzene-d$_4$.

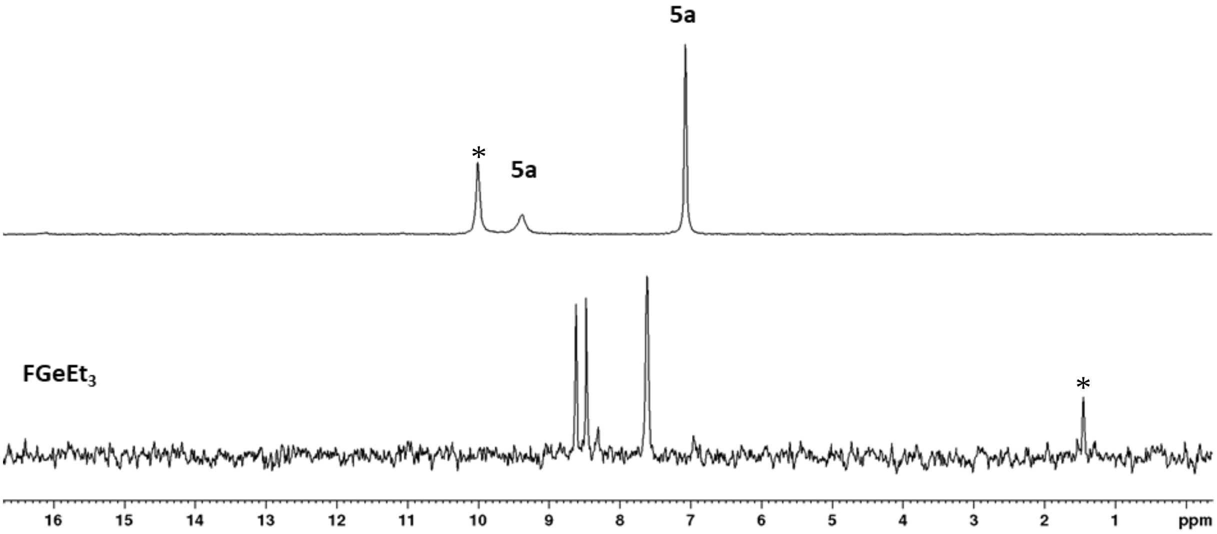

Figure S22. Section of the $^{13}C\{^1H\}$ NMR spectra of Et_3GeF (bottom) and $[Et_3GeFGeEt_3][B(C_6F_5)_4]$ (**5a**, top) in *o*-dichlorobenzene-d_4. * Impurity.

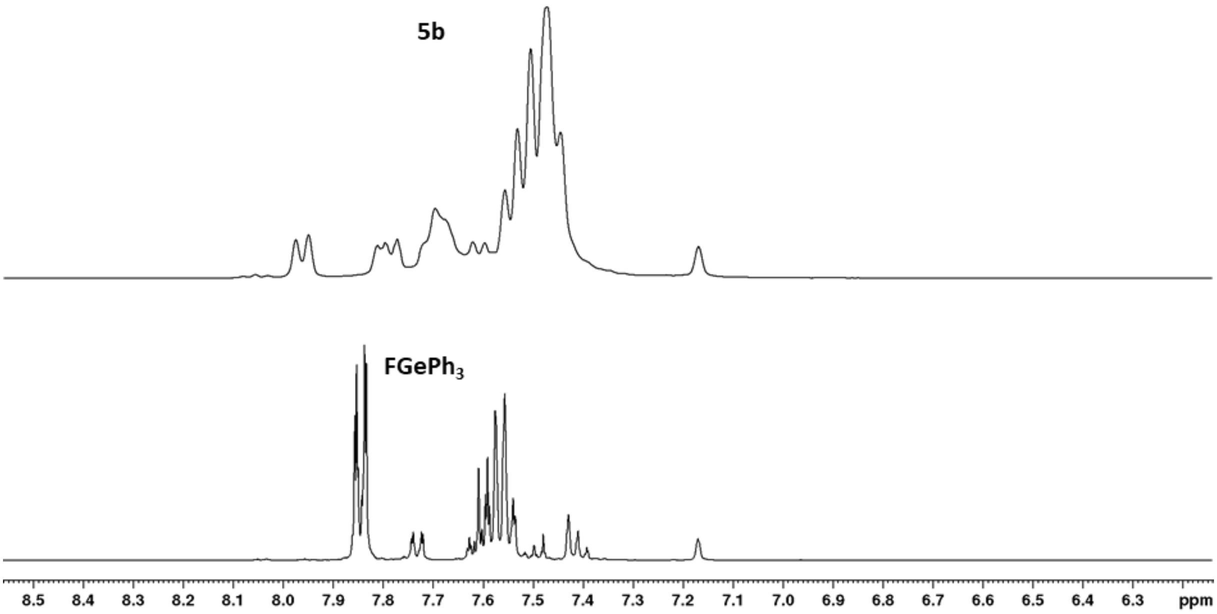

Figure S23. ^1H NMR spectra of Ph_3GeF (bottom) and $[Ph_3GeFGePh_3][B(C_6F_5)_4]$ (**5b**, top) in *o*-dichlorobenzene-d_4. Note that C_6D_6 was not completely removed.

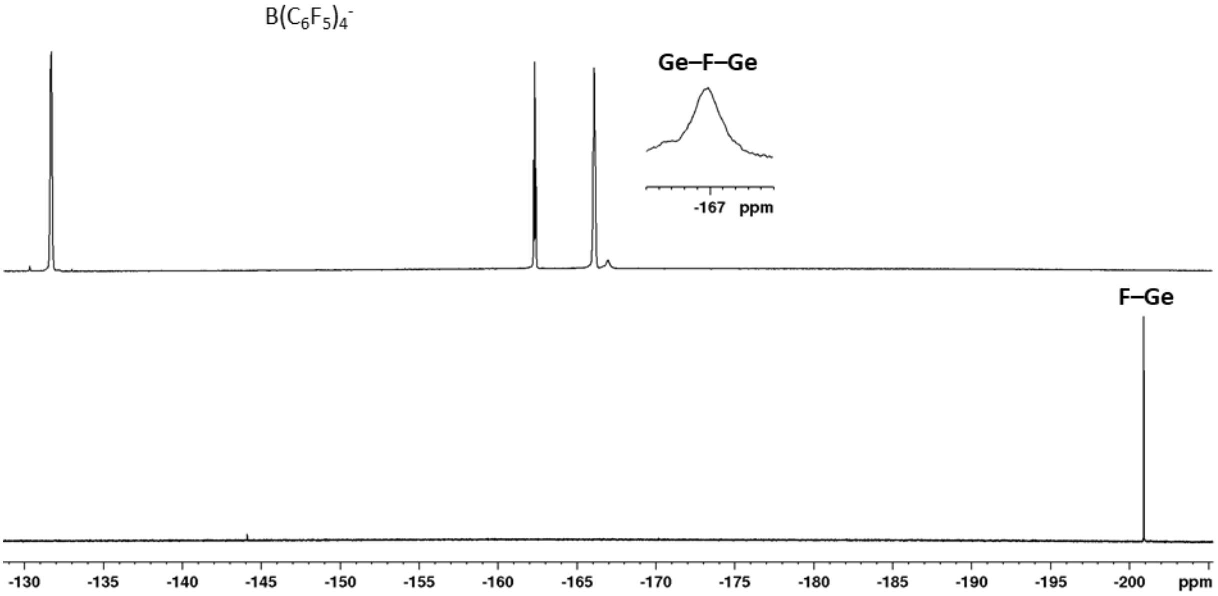

Figure S24. ^{19}F NMR spectra of Ph_3GeF (bottom) and $[Ph_3GeFGePh_3][B(C_6F_5)_4]$ (**5b**, top) in *o*-dichlorobenzene-d_4.

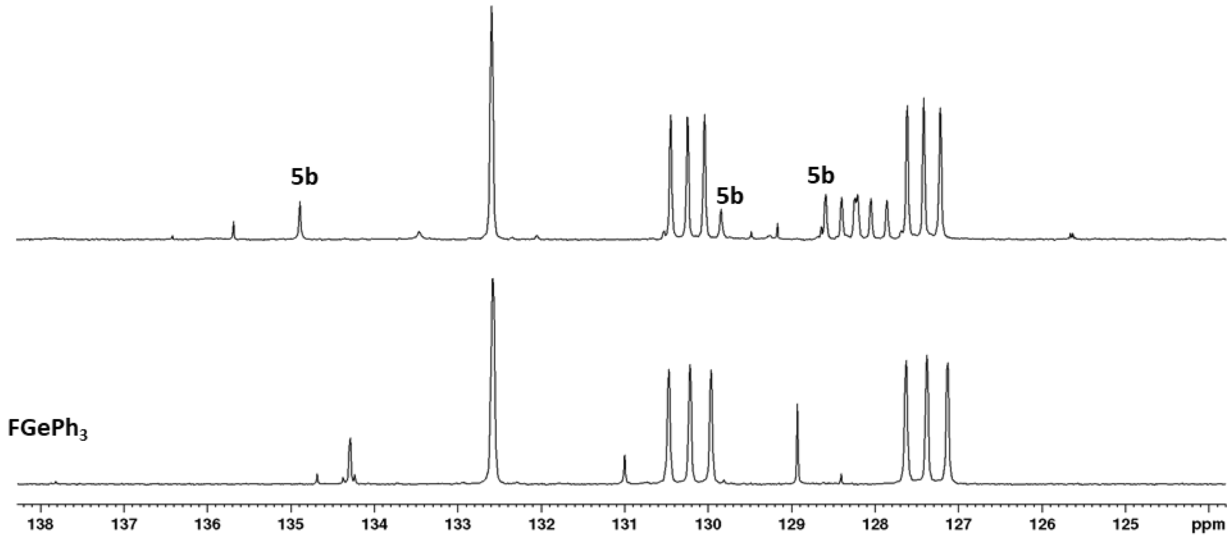

Figure S25. $^{13}C\{^1H\}$ NMR spectra of Ph_3GeF (bottom) and $[Ph_3GeFGePh_3][B(C_6F_5)_4]$ (**5b**, top) in *o*-dichlorobenzene-d_4. Note that C_6D_6 was not completely removed.

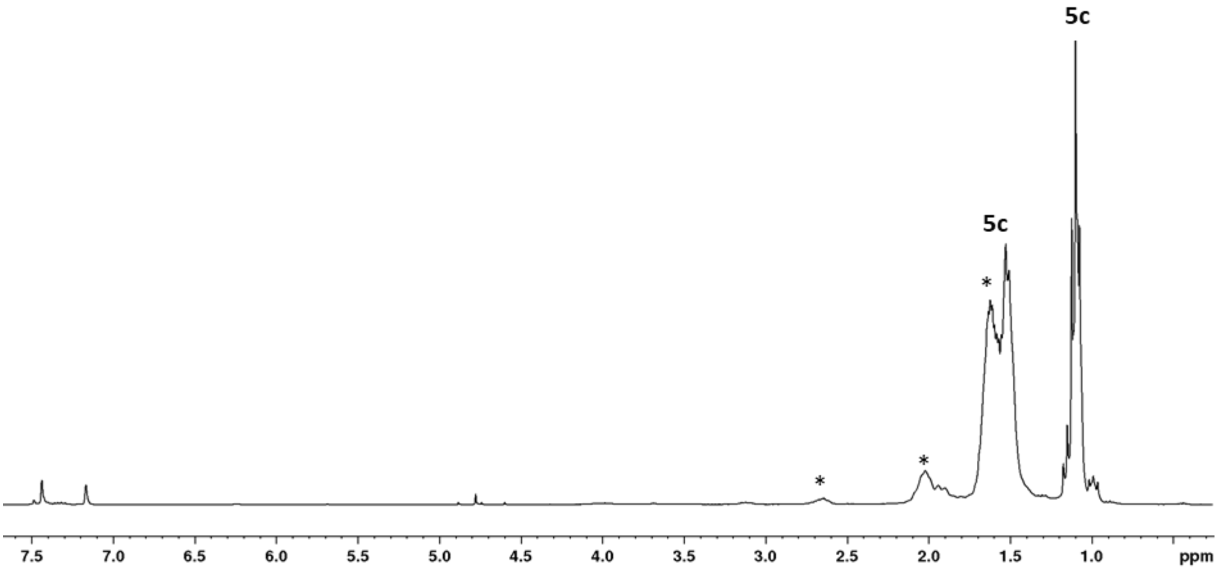

Figure S26. ^{1}H NMR spectrum of the reaction of **2c** and fluorocyclohexane to form [*n*Bu$_3$Ge-F-Ge*n*Bu$_3$][B(C$_6$F$_5$)$_4$] (**5c**) in *o*-dichlorobenzene-d$_4$. Note that C$_6$D$_6$ was not completely removed. * = 1,2-dichloro-4-cyclohexylbenzene-d$_3$.

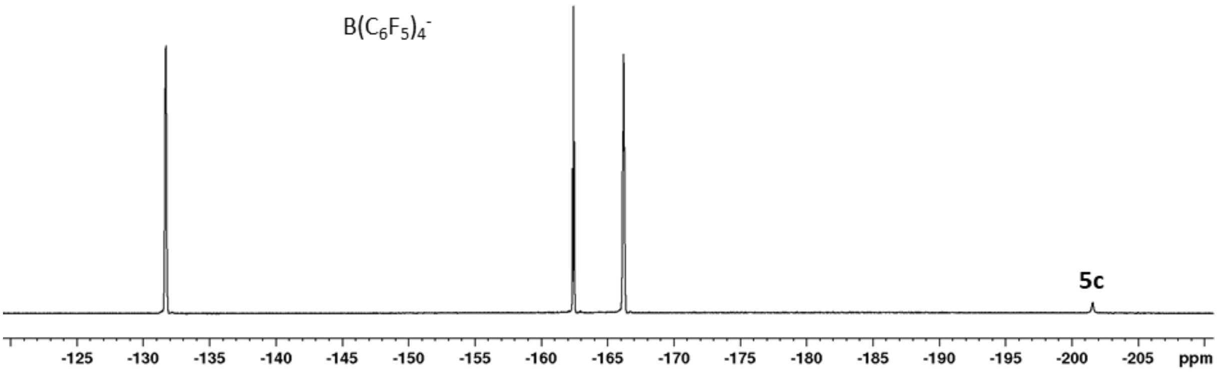

Figure S27. ^{19}F NMR spectrum of the reaction of **2c** and fluorocyclohexane to form [*n*Bu$_3$Ge-F-Ge*n*Bu$_3$][B(C$_6$F$_5$)$_4$] (**5c**) in *o*-dichlorobenzene-d$_4$.

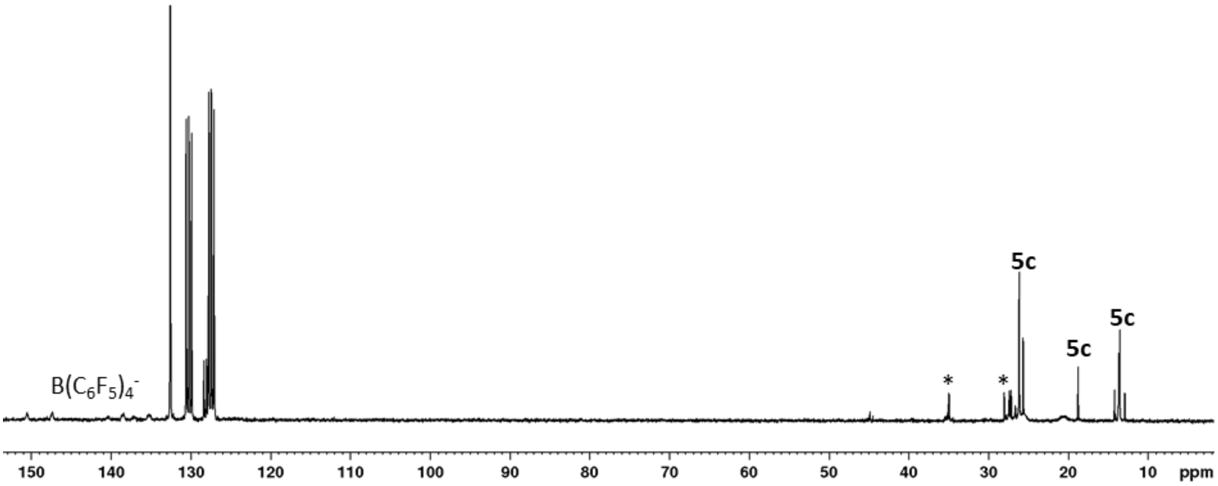

Figure S28. ^{13}C{^{1}H} NMR spectrum of the reaction of **2c** and fluorocyclohexane to form [*n*Bu$_3$Ge-F-Ge*n*Bu$_3$][B(C$_6$F$_5$)$_4$] (**5c**) in *o*-dichlorobenzene-d$_4$. Note that C$_6$D$_6$ was not completely removed. * = 1,2-dichloro-4-cyclohexylbenzene-d$_3$.

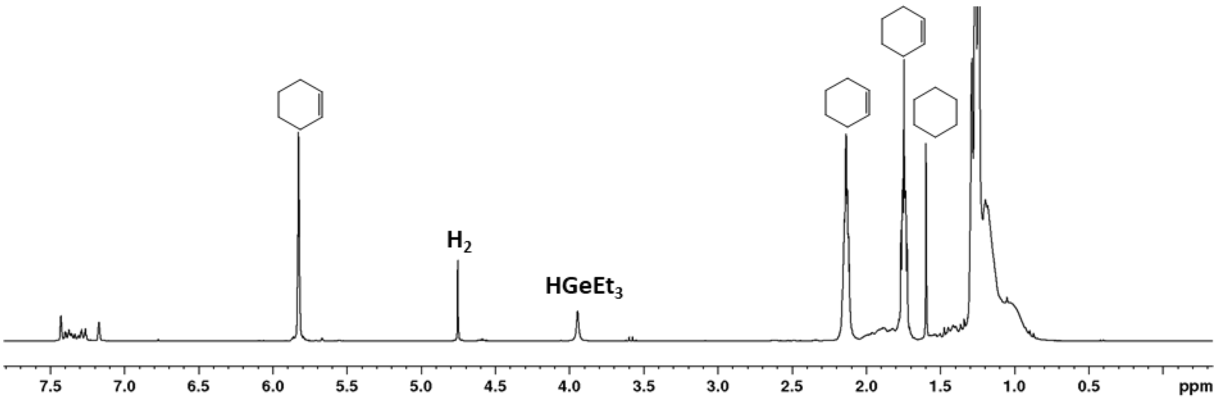

Figure S29. ^{1}H NMR spectrum of the catalytic dehydrofluorination of fluorocyclohexane in *o*-dichlorobenzene-d$_4$.

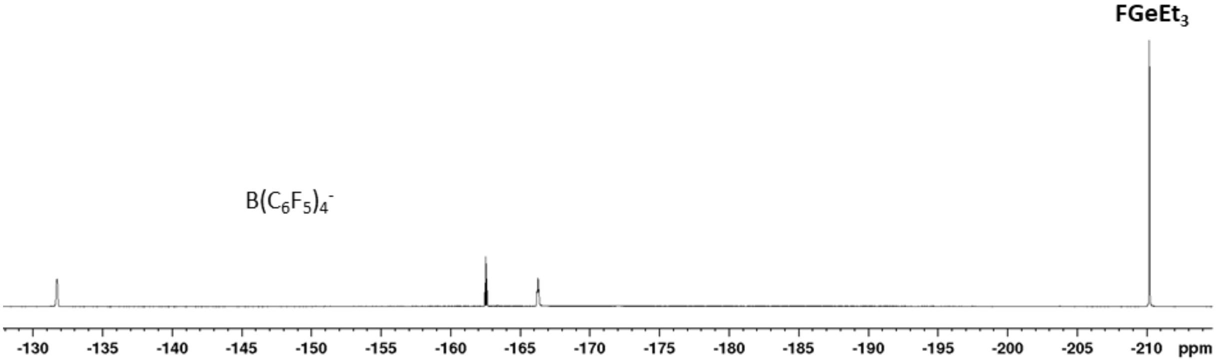

Figure S30. ^{19}F NMR spectrum of the catalytic dehydrofluorination of fluorocyclohexane in *o*-dichlorobenzene-d$_4$.

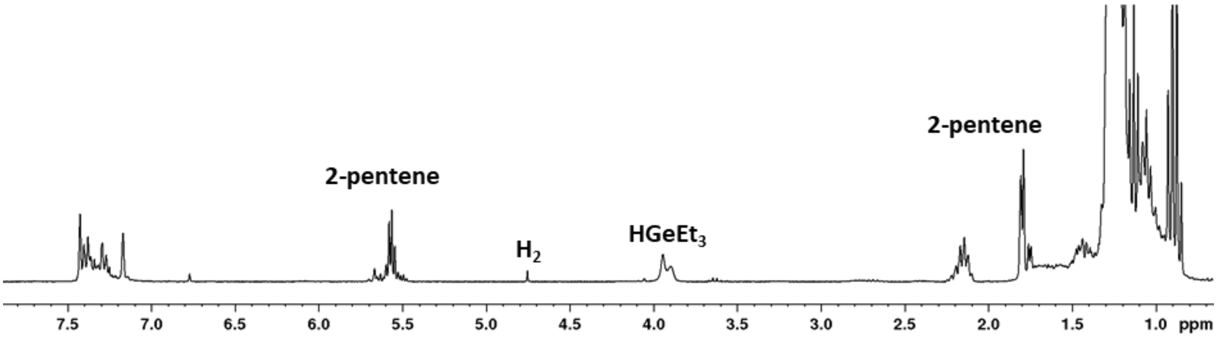

Figure S31. ^{1}H NMR spectrum of the catalytic dehydrofluorination of fluoropentane in *o*-dichlorobenzene-d$_4$.

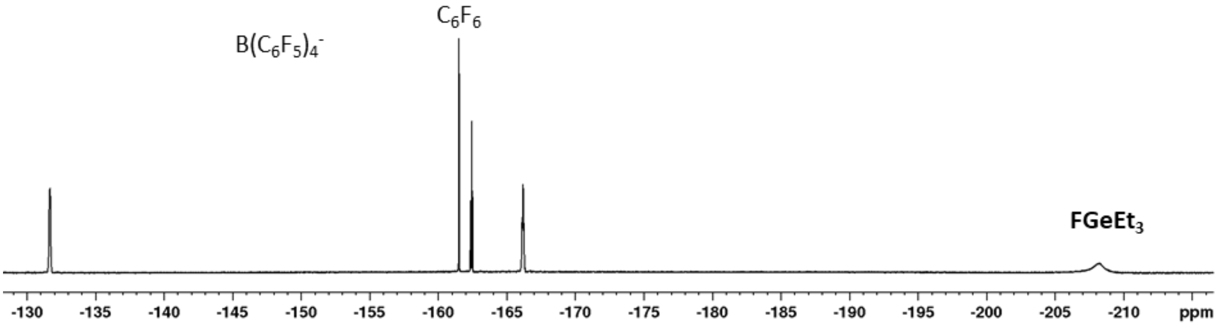

Figure S32. ^{19}F NMR spectrum of the catalytic dehydrofluorination of fluoropentane in *o*-dichlorobenzene-d_4. C_6F_6 was used as standard.

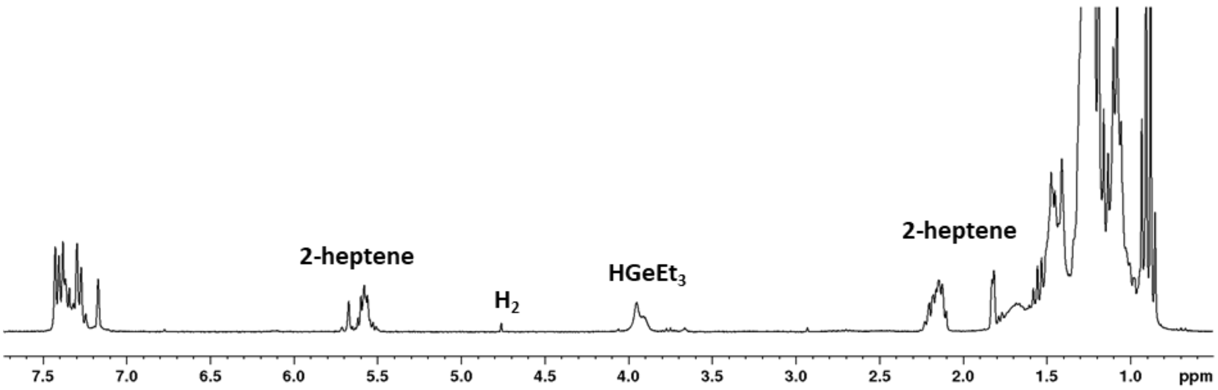

Figure S33. ^1H NMR spectrum of the catalytic dehydrofluorination of fluoroheptane in *o*-dichlorobenzene-d_4.

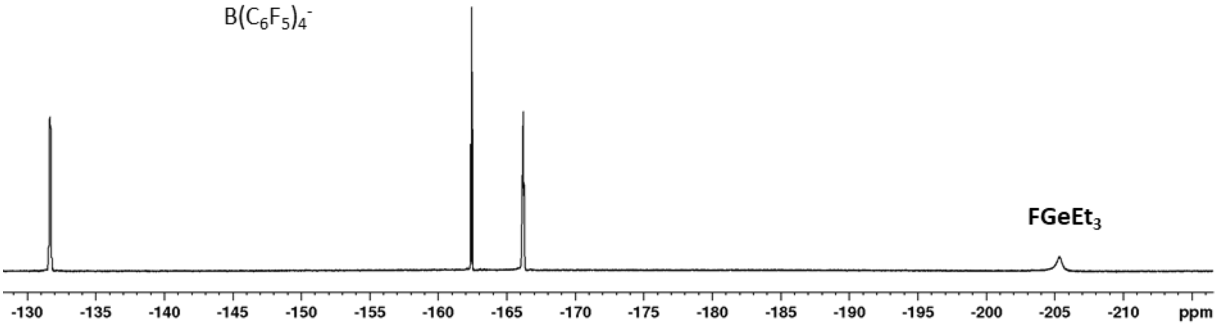

Figure S34. ^{19}F NMR spectrum of the catalytic dehydrofluorination of fluoroheptane in *o*-dichlorobenzene-d_4.

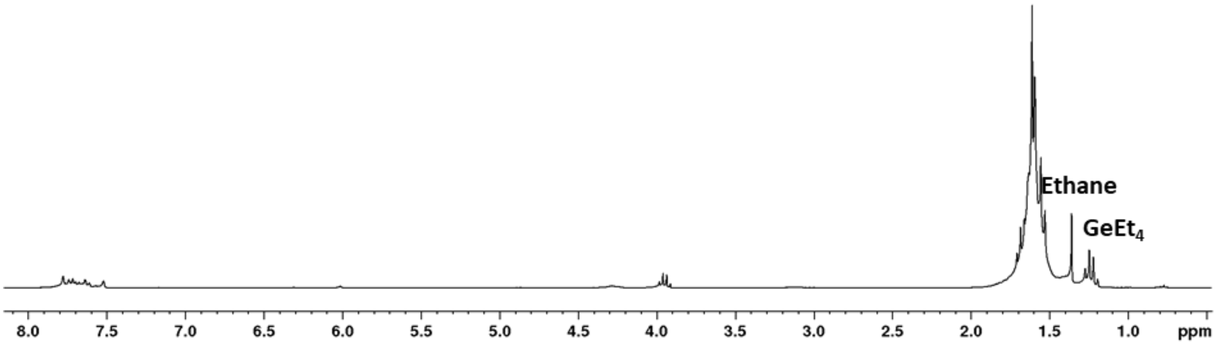

Figure S35. ^{1}H NMR spectrum of the activation of fluoroethane in *o*-dichlorobenzene-d$_4$.

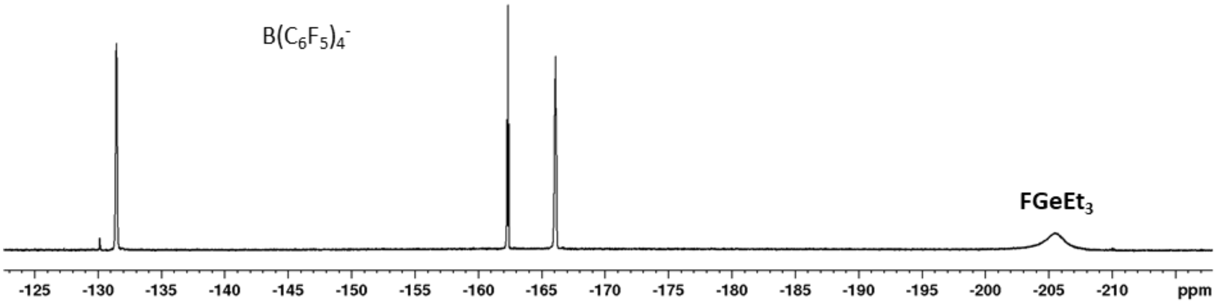

Figure S36. ^{19}F NMR spectrum of the activation of fluoroethane in *o*-dichlorobenzene-d$_4$.

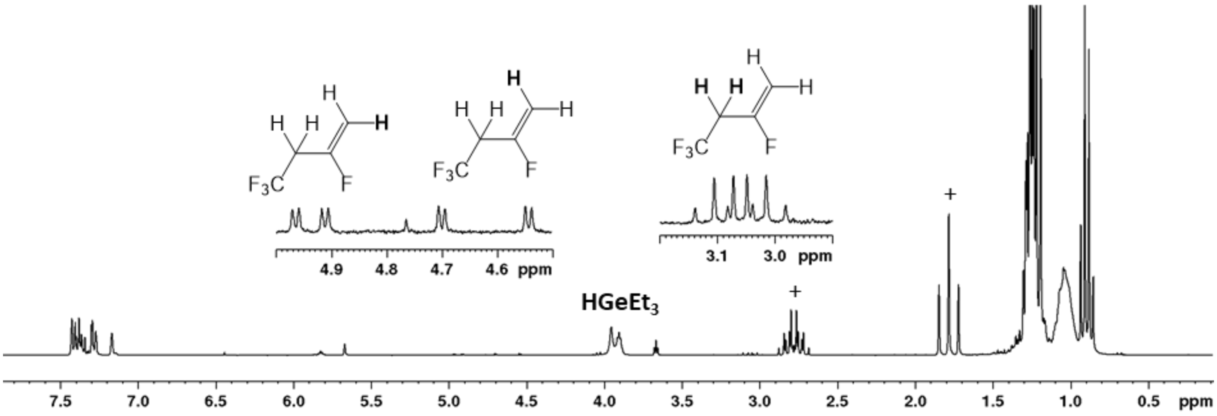

Figure S37. ^{1}H NMR spectrum of the dehydrofluorination of 1,1,1,3,3-pentafluorobutane (+) in *o*-dichlorobenzene-d$_4$.

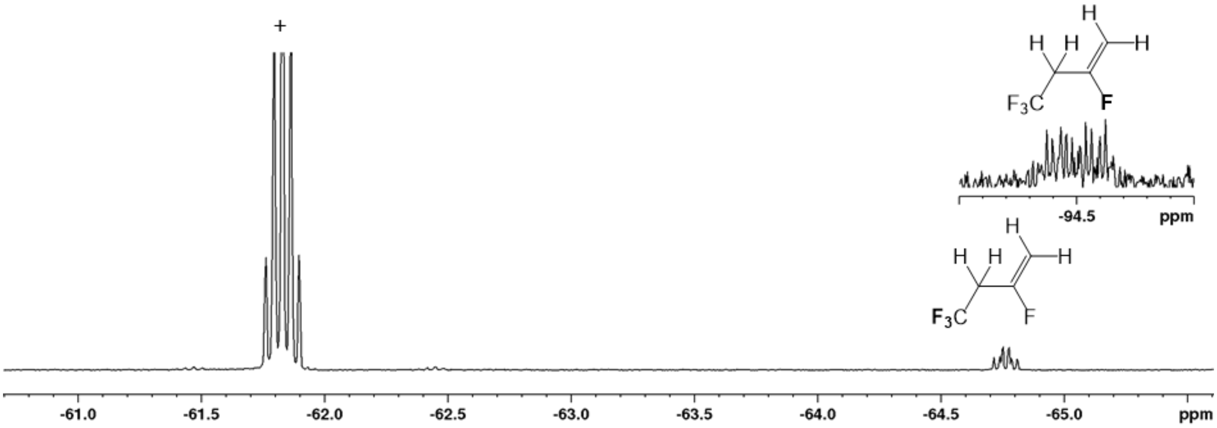

Figure S38. Section of the ^{19}F NMR spectrum of the dehydrofluorination of 1,1,1,3,3-pentafluorobutane (+) in *o*-dichlorobenzene-d4.

7. References

[1] S. Popov, B. Shao, A. L. Bagdasarian, T. R. Benton, L. Zou, Z. Yang, K. N. Houk and H. M. Nelson, *Science*, **2018**, *361*, 381-387.

[2] G. M. Sheldrick, *SADABS*, Program for Empirical Absorption Correction, Version SADABS-2014/5, Bruker Analytical X-ray Systems, Madison, WI, USA, **2011**.

[3] G. M. Sheldrick, *SHELXT-2014*, Program for Crystal Structure Solution, University of Göttingen, Germany, **2013**; G. M. Sheld-rick, *SHELXL-2013*, Program for Crystal Structure Refinement, University of Göttingen, Germany, **2013**.